Effects of forest fire smoke and volcanism on the stratospheric aerosol

Sandvik, Oscar

2021

Document Version:
Publisher's PDF, also known as Version of record

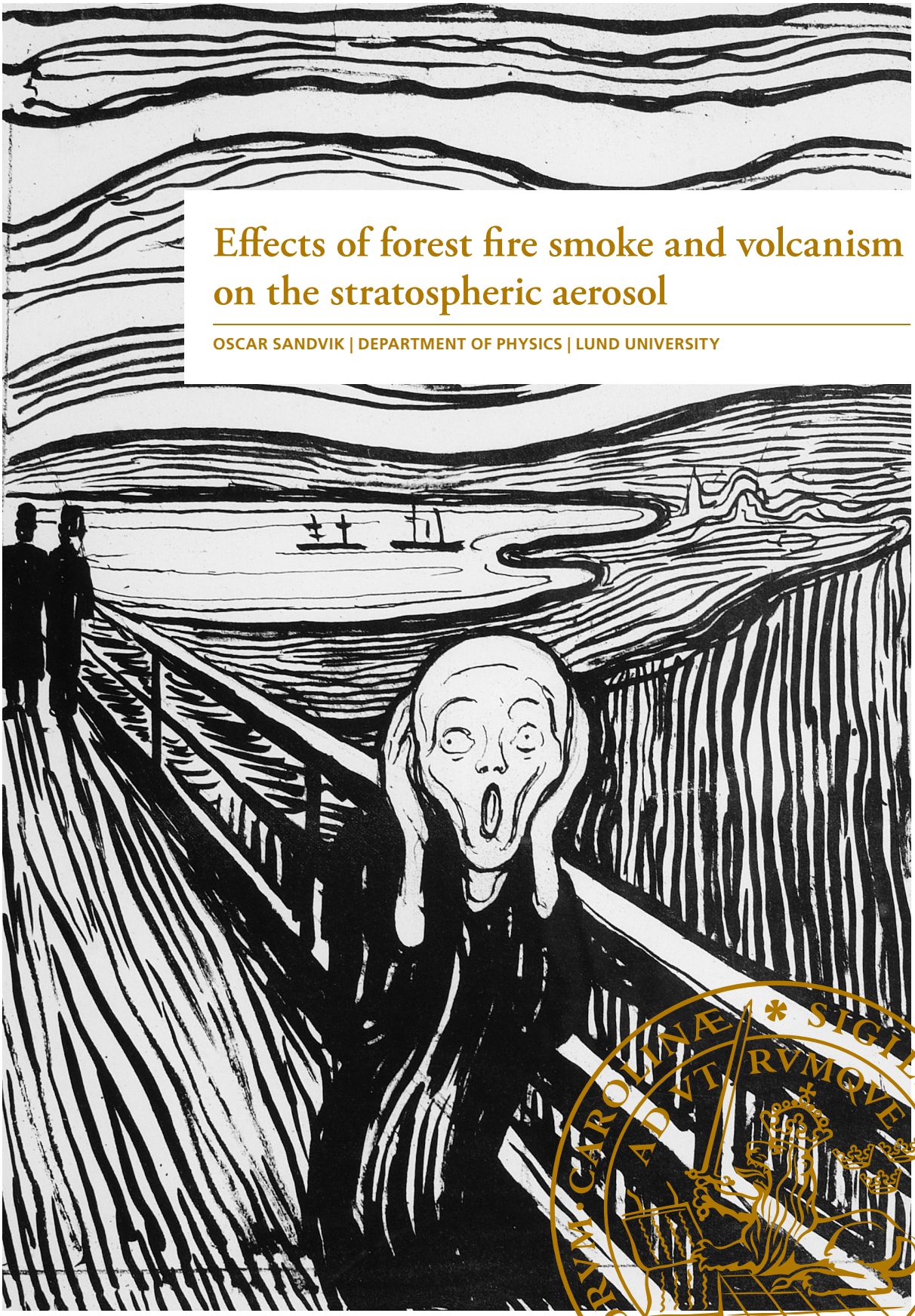

Effects of forest fire smoke and volcanism on the stratospheric aerosol

OSCAR SANDVIK | DEPARTMENT OF PHYSICS | LUND UNIVERSITY

Oscar Sandvik got his master's degree in Engineering Physics in 2016. Immediately after that, he started his PhD. The stratospheric aerosol and how it is perturbed by volcanic eruptions and forest fires are the focus of this thesis. Measurements of this aerosol were obtained by satellite instruments and in-situ aircraft samples. The research involved in this thesis has involved many terabytes of data, which have been analysed using Python and Matlab. While not doing research, Oscar has taught university students and digitalised laboratory exercises during the present pandemic.

Printed by Media-Tryck, Lund 2021 NORDIC SWAN ECOLABEL 3041 0903

LUND UNIVERSITY

Faculty of Engineering
Department of Physics

ISBN 978-91-7895-765-1

Effects of forest fire smoke and volcanism on the stratospheric aerosol

Effects of forest fire smoke and volcanism on the stratospheric aerosol

Oscar Sandvik

LUND
UNIVERSITY

DOCTORAL DISSERTATION

by due permission of the Faculty of Engineering, Lund University, Sweden.
To be defended at Rydbergssalen, Fysicum. Date: 2021-03-19. Time 09:15.

Thesis supervisors
Prof. Bengt Martinsson, Dr. Johan Friberg, Dr. Moa Sporre and Dr. Göran Frank

Faculty opponent
Dr. Claudia Timmreck

Organization	Document name
LUND UNIVERSITY	DOCTORAL DISSERTATION
	Date of issue 2021-03-19
Author Oscar Sandvik	Sponsoring organization

Title and subtitle
Effects of forest fire smoke and volcanism on the stratospheric aerosol

Abstract

This thesis explores the stratospheric aerosol through both in-situ measurements and remote sensing. The background stratospheric aerosol is complex and is perturbed by injections of forest fire smoke particles and by particles formed from volcanic SO2. Climate models need accurate description of the stratospheric aerosol in order to have sound radiation budgets. Using the remote sensing technique of satellite borne lidar, it was seen that volcanic eruptions increased the stratospheric optical depth on average by 40 % in the period between 2006 and 2015. Forest fires also increased the stratopheric optical depth but their effect was found to dissapear faster than the effect from volcanic eruptions. By investigating in-situ samples, the background aerosol was found to contain a carbonaceous fraction that seems to be produced in the stratosphere. In order to better portray fresh volcanic emissions of SO2, a new method of compiling SO2 datasets with high vertical resolution was developed. This method combined many lidar observations of the aerosol formed from SO2 to provide vertical distributions of the SO2 gas. The lidar used in this thesis is CALIOP which is aboard the CALIPSO satellite. The satellite was launched in 2006 and CALIOP is still operational. This lidar measures the radiation scattering from the aerosol at a high vertical resolution. Measurement of elemental concentrations and other in-situ measurements were done using the IAGOS-CARIBIC aircraft platform. Both CALIOP and IAGOS-CARIBIC have long successful histories of measurements which allowed long-term effects to be studied. A comparison between the in-situ measurements from IAGOS-CARIBIC and the remote sensing measurements by CALIOP was also made. If the measurements are taken sufficently above the tropopause, then the the calculated scattering based on in-situ IAGOS-CARIBIC measurements of sulphur, water and carbon are similar to the scattering measured by CALIOP. In the vicinity of the tropopause, additional aerosol components and water uptake are needed to explain the scattering from stratospheric aerosol.

Key words Remote sensing, stratospheric aerosol, forest fire smoke, volcanism, CALIOP, FLEXPART, CALIPSO, AIRS, IAGOS-CARIBIC

Classification system and/or index terms (if any)

Supplementary bibliographical information	**Language** English
ISSN and key title	**ISBN** 978-91-7895-765-1 (print) 978-91-7895-766-8 (pdf)

Recipient's notes	**Number of pages** 64	Price
	Security classification	

Signature Oscar Sandvik Date 2020-02-08

Effects of forest fire smoke and volcanism on the stratospheric aerosol

Oscar Sandvik

LUND
UNIVERSITY

Coverphoto by Edvard Munch (Public Domain). It has been suggested that Munch was inspired to paint the scream by the blood-red sunsets caused by the 1883 Krakatau eruption.

Faculty of Engineering, Department of Physics

ISBN: 978-91-7895-765-1 (print)
ISBN: 978-91-7895-766-8 (pdf)

Printed in Sweden by Media-Tryck, Lund University
Lund 2021

Media-Tryck is a Nordic Swan Ecolabel certified provider of printed material. Read more about our environmental work at www.mediatryck.lu.se

MADE IN SWEDEN

Table of Contents

List of publications and author's contributions **9**

Publications not included in this thesis **11**

Acknowledgements **13**

Populärvetenskaplig sammanfattning **15**

Aim of Research **17**

Introduction **19**

Volcanoes 19

Aerosols 20

Primary and secondary aerosols 22

Health impact 22

Sources to stratospheric aerosols 22

Background 22

Volcanic 24

Forest fires 25

Stratospheric height coordinates 26

Geometric altitude and geopotential height 26

Potential vorticity 26

Potential temperature isentropes 26

Atmospheric structure 27

Tropopause 28

Stratosphere 30

Lowermost Stratosphere 30

Stratospheric dynamics 31

Brewer Dobson circulation 31

Isentropic transport 32

Asian Tropopause Aerosol Layer (ATAL) 32

Subtropical jet 33

Methods **35**
Remote sensing 35
CALIOP 35
AIRS 39
OMI 40
In-situ observations 40
IAGOS-CARIBIC 40
Meteorological reanalysis 42
FLEXPART 42
Findings **45**
Background aerosol 45
Volcanic aerosol 47
Forest fire aerosol 50
Vertical structure 51
Conclusion **53**
Outlook **55**
References **57**

List of publications and author's contributions

Paper I: Friberg, J., Martinsson, B. G., Andersson, S. M., and Sandvik, O. S.: Volcanic impact on the climate – the stratospheric aerosol load in the period 2006–2015, Atmos. Chem. Phys., 18, 11149-11169, 10.5194/acp-18-11149-2018, 2018.

I worked with the data analysis techniques and discussed the contents of the manuscript throughout the writing and review processes.

Paper II: Martinsson, B. G., Friberg, J., Sandvik, O. S., Hermann, M., van Velthoven, P. F. J., and Zahn, A.: Formation and composition of the UTLS aerosol, npj Climate and Atmospheric Science, 2, 10.1038/s41612-019-0097-1, 2019.

I discussed the contents of the manuscript throughout the writing and review processes. I also worked on the ion beam analytical tasks.

Paper III: Sandvik, O. S., Friberg, J., Martinsson, B. G., van Velthoven, P. F. J., Hermann, M., and Zahn, A.: Intercomparison of in-situ aircraft and satellite aerosol measurements in the stratosphere, Sci. Rep., 9, 15576, 10.1038/s41598-019-52089-6, 2019.

I wrote the paper, did the data analysis, produced the figures and interpreted the results.

Paper IV: Martinsson et al. 2021 (manuscript) – Rapid decline of wildfire smoke in the stratosphere

I made the initial data analysis and filtering. I also discussed the contents of the manuscript throughout the writing and first review processes.

Paper V: Sandvik et al. 2021 (manuscript) - Methodology to obtain vertically resolved SO_2 data for representation of volcanic emissions in climate models

I created the method used in the study, produced the figures, interpreted the results and wrote the manuscript.

Publications not included in this thesis

Martinsson, B. G., Friberg, J., Sandvik, O. S., Hermann, M., van Velthoven, P. F. J., and Zahn, A.: Particulate sulfur in the upper troposphere and lowermost stratosphere – sources and climate forcing, Atmos. Chem. Phys, 17, 10937-10953, 10.5194/acp-17-10937-2017, 2017.

Acknowledgements

First I want to thank my wife Lina, my mother Annette, my father Mats and my brother Anton who have been supportive through this whole process.

Bengt for being a great advisor and helping me with everything.

My co-advisor Johan for always giving me new ideas.

My co-advisor Moa for nice discussion and for being mine and Lina's personal wedding meteorologist.

Elisabet, Lars and Jonas as Lina's supportive family who have helped us tremendously during these years.

Co-advisor Göran for helping me with the administrative things.

My office mates Nathaly, Anton, Nicolai and Yuliia for being great company and keeping the office nice and lush with plants from floor to ceiling.

Pico for bringing great coffee from Colombia and for nice chats.

Markus for discussing the stock and lunch market.

Dirk for keeping the division afloat.

Charlotta for nice conversations and someone to discuss the many quirks of this building.

Hanno for bringing nice board-games.

Francesco for nice lunch discussions.

Guillaume and Danny for the cheese supplies for fondue evenings.

Mikael for helping out with the IT things.

Emil and Alexander for the nice discussions.

Pontus and Adam for the aerosol courses.

Python, xarray, matplotlib and cartopy for being awesome open-source projects aiding my data analysis.

Populärvetenskaplig sammanfattning

Om det ej råder balans mellan den strålning som kommer till jorden och den strålning som lämnar jorden kommer jordens temperatur att förändras. Ett välkänt exempel är de förhöjda nivåerna av växthusgaser som leder till att strålning från jorden får det svårare att försvinna ut till rymden. Resultatet av detta blir att energin stannar kvar vid jorden och temperaturerna stiger. Vi är alla bekanta med att molnighet under en varm sommardag sänker temperaturen. Molnen reflekterar bort det inkommande solljuset. På samma sätt kan små partiklar som finns i atmosfären också reflektera bort inkommande solljus. Dessa partiklar kan komma från flera olika källor, till exempel: de kan bildas utifrån gaser i atmosfären, de kan vara rökpartiklar från skogsbränder och de kan komma från vulkanutbrott.

Vulkaner kan få storlagna utbrott med mängder av magma och het aska som väller ut. Från en av gaserna, svaveldioxid, som kommer ur vulkaner kan små partiklar bildas och dessa partiklar reflekterar solljus. Det som kommer upp kommer till slut ned och dessa partiklar påverkar temperaturen endast under en begränsad tid. Denna tid kan dock vara flera år lång och om flera tillräckligt stora vulkanutbrott sker nära inpå varandra blir det som en lång utdragen tid av kallare temperaturer.

Atmosfären är uppdelad i lager. De flesta väderfenomen sker i det understa lagret, som kallas för troposfären. Ovanför troposfären ligger stratosfären, det är här det mesta av ozonen finns. Här finns även ett mindre känt lager med små svavelpartiklar som heter Junge-lagret. I stratosfären finns knappt några moln och anledningen är att vid gränsen mellan stratosfären och troposfären, som kallas för tropopausen, är det mycket kallt. Kylan gör den till en barriär för det mesta utav vattenångan som fryser fast på molnpartiklar innan den kan nå upp till stratosfären. Både ovanför och under tropopausen är det varmare än vid tropopausen vilket försvårar för luften att passera den.

Ett vulkaniskt moln är en utmaning att följa. Askan kan man oftast se med blotta ögat men för svaveldioxiden behöver man speciella mätinstrument. När molnet sträcks ut behöver man speciella instrument även för askan. Eftersom molnen kan färdas runt hela jordklotet behöver man sätta instrumenten antingen utspridda över hela världen eller sätta dem på flygplan eller satelliter som klarar av att följa molnen under deras långa

färd. Med hjälp av datorsimuleringar kan man också beräkna hur molnen kan väntas förflytta sig givet att man har tillförlitliga meteorologiska prognoser. Ofta är forskare instresserade av att undersöka speciellt stora moln och då försöker man sammanställa de mätningar som gjorts och göra datorsimuleringar. Dessa simuleringar drivs av sammanställda meteorologiska data vilka kallas för meteorologiska omanalyser.

Vart de vulkaniska molnen tar vägen beror både på var utbrottet sker och till vilken höjd molnet når. Aska faller oftast snabbt ner i regionen runt omkring vulkanen. Svaveldioxid bildar surt regn om utbrottsmolnet håller sig i troposfären. Detta sker genom att svaveldioxiden tas upp av vattendroppar och blir till små svavelsyrapartiklar. Om svaveldioxiden tog sig hela vägen upp till stratosfären oxideras de till svavelsyra och bildar sen ännu mindre svavelpartiklar. Väl uppe i stratosfären kan dessa pyttesmå svavelpartiklar stanna i flera månader eller till och med år. Anledningen till detta är att gravitationen drar svagt i partiklarna och att partiklarna kan transporteras uppåt av vindar.

Det finns idéer om att man skulle kunna skapa konstgjorda partiklar som liknar de vulkaniska partiklarna för att motverka den globala uppvärmningen. Det har aldrig prövats förut och det finns fortfarande kunskapsluckor kring hur partiklar transporteras i stratosfären.

De senaste åren har vi kunnat se enorma skogsbränder runt om i världen. Dessa bränder har varit såpass stora att de liknar vulkaniska utbrott i omfattning. Brandplymerna kan också lyfta partiklar upp till stratosfären. Dock har partiklarna från skogsbränderna en annan kemisk sammansättning än de vulkaniska partiklarna med mer organiskt material och är i grunden sotpartiklar. Detta gör att de kan stiga lite extra genom uppvärmning från solens strålar. Denna strålning kan också leda till att de bryts ned. Fler stora skogbränder är att vänta sig i takt med att den globala medeltemperaturen ökar och vi får varmare somrar.

Min forskning har fokuserat på hur de stratosfäriska partiklarna bildas och transporteras, hur man kan avgöra deras position samt vad de stratosfäriska partiklarna består av. Det finns idag många satelliter och mätplattformar för att mäta detta. Dock har de en begränsad mängd av perspektiv: vissa kanske har en bra horisontell upplösning i sin data men saknar uppfattning om höjdprofilen, andra har den motsatta uppsättningen. Att väva ihop data från flera plattformar har därför varit grundstommen i denna avhandling och därför har mycket tid och möda lagts ned på att förstå mätteknikerna i grunden och att hitta lämpliga metoder för sammansätta datan på nya mer detaljerade sätt.

Aim of Research

The aim of the research for this thesis has been to better understand the stratospheric aerosol. In order to properly model the Earth's surface temperatures, one needs to include volcanic aerosol particles in the stratosphere that partially reflect incoming solar radiation back to space before it reaches the surface (Santer et al., 2014). There is a complex mixture of aerosol particles in the stratosphere, even during background conditions. Every now and then, events at the surface lead to additional particles in the stratosphere, such as large forest fires and volcanic eruptions. Before the additional particles descend and disappear on the lower side of the tropopause, they reside in the lowermost stratosphere. This part of the stratosphere has been neglected in climate models (Andersson et al., 2015). For climate models to properly take aerosols into account, they need to have accurate knowledge of the time, location and mechanisms of the aerosol particles. For the stratospheric aerosol to be better characterized, the following aspects have been studied:

- The formation and composition of the stratospheric aerosol during background conditions.
- The transport of aerosol particles within, and out of, the stratosphere.
- The perturbation of the stratospheric aerosol by forest fires and volcanism, and the new particles' evolution and decay.
- The long-term effect from volcanism on the stratospheric aerosol.
- The correlation between in-situ and remote sensing measurements, specifically those on radiation scattering from the stratospheric aerosol.
- The vertical distribution of emitted aerosol pre-cursor SO_2 from volcanic eruptions and how vertical distributions can be determined by combining lidar data with trajectory modelling.

Introduction

This thesis encapsulates more than four years of study of stratospheric aerosol particles and aims to put the authored papers into the context of the field. First the sources of the aerosol particles are presented. Secondly, the stratosphere is presented by explaining how it is defined and how matter is transported to and from it. After this, the instruments and methods which have been used to observe the aerosol particles are presented. Finally, the findings of several studies are discussed together with an outlook for future research.

Volcanoes

A volcanic plume is not smoke from the magma but made out of small pieces from the volcano called tephra. Volcanoes are also big emitters of gas even though this is harder to observe. Most of the volcanic gas emissions consist of CO_2, SO_2 and H_2O. Even though volcanoes emit a lot of CO_2 they don't even compare with human emissions of this gas. SO_2 is a completely different story and is the main topic of this thesis. SO_2 is a well-known pollutant, smelling like rotten eggs. It is hazardous to inhale and is emitted in fossil fuel combustion. The SO_2 from volcanic eruptions can be lifted high up in the atmosphere, so high in fact that clouds won't remove it through rain drop formation. Instead when the SO_2 is above the clouds, it remains longer and can be converted into gaseous sulphuric acid. The gaseous sulphuric acid and the scarce H_2O at high altitudes condenses onto pre-existing particles, and forms what is called sulphate aerosol. The sulphate aerosol has the interesting physical property that it reflects incoming sunlight. This in turn cools surface temperatures. There is also a chance that Munch was inspired to paint the Scream because of the blood-red sunsets after the 1883 Krakatau eruption (Olson et al., 2004).

One of the largest eruptions in recent centuries was the eruption of Tambora in 1815. The aerosol from that eruption caused such immense cooling that the year after the eruption was called "the year without summer", with the effect of crop failures (Robock, 2000).

A modern example of a very large eruption is the eruption of Mt. Pinatubo in 1991. Mount Pinatubo is located in the tropics, which meant that the sulphate aerosol could spread into both the northern and the southern hemisphere. This led to a 0.7 °C drop in tropospheric temperature the following year (McCormick et al., 1995).

Almost everyone knows of the Eyjafjallajökull eruption in 2010. But because there was mostly ash in the eruption plume and that the plume did not reach the stratosphere, this eruption had negligible effect on the climate. The eruption did however have a large impact on aircraft safety in Europe, with the result of many grounded flights, and is another reason for careful monitoring of volcanic emissions. This eruption is a good example of when the visible ash plume takes the spotlight from the sulphur dioxide which is only "visible" in the ultraviolet and infrared spectrum. A year later, Grimsvötn erupted and released much more SO_2 (Flemming and Inness, 2013).

In the year 2009 on a small Kuril island, the volcano Sarychev volcano erupted during several days in multiple eruptions. The Sarychev eruption emitted 1.2 Tg of SO_2 (Haywood et al., 2010). The SO_2 from this eruption also entered the stratosphere and the resulting aerosol spread over the northern hemisphere. In papers I and III, the effects of volcanism on scattering over long time spans (2006 to 2015) were studied. In this time interval, the Sarychev eruption is clearly visible. Due to the several eruptions from Sarychev reaching different altitudes, the vertical distribution of the emitted SO_2 was studied in paper V.

Aerosols

An aerosol is particles suspended in a gas. The whole atmosphere can be seen as an aerosol with more or fewer particles at different times and locations. Usually, one defines an aerosol being within a smaller volume. The particles in an aerosol have diameters between 1-3 nm (one billionth of a meter) and 100 µm (0.1 mm). Anything smaller than this interval are just gas molecules or unstable clusters of molecules. If the diameter of a particle is larger than the size interval, then gravity will pull down the particle too much for it to be able to stay suspended for any meaningful time.

Aerosol particles released by humans can have an effect on climate by blocking sunlight, which is called the direct effect. They can also impact the climate by altering the reflectivity of clouds, which is called the indirect effect. The reflectivity change comes from that a higher number of aerosol particles leads to a higher number of smaller cloud droplets which increases the reflectivity and thus cools the climate. Another indirect

effect that has been theorized is that a higher number of cloud particles would increase the lifetimes of clouds and by delayed rainfall since the cloud droplets are smaller.

Soot particles or particles with a high carbon content are labelled as “black carbon”. These particles have a broad absorption spectrum and they warm the atmosphere by absorbing radiation otherwise scattered by clouds, aerosol particles and the surface (Ramanathan and Carmichael, 2008). The size of this effect is uncertain, but counteracts some of the cooling by other aerosol particles. The unbalance in radiation caused by additional aerosol or gases is called radiative forcing. This unbalance leads to either cooling or warming of the climate. There are many different sources for the aerosols at the different layers of the atmosphere, some of these are shown in Fig. 1.

The uncertainty concerning aerosol particles’ radiative forcing is still relatively large compared to that of greenhouse gases. However, in absolute numbers the aerosols have still a much smaller radiative forcing than greenhouse gases. It is just that their precise radiative forcing is harder to pin down. As of now, aerosol’s radiative forcing has the most uncertainty of the forcing agents (see Fig. TS.6 in IPCC (2013)).

The effect of aerosols is much shorter compared to that of greenhouse gases. But sustained large emissions from either volcanoes or humans can be long lasting and cumulative and thus lead to an overall effect relevant for the climate. If atmospheric models don’t account for the effect of aerosols, then they can provide false predictions. Volcanic sulphate aerosol particles in the stratosphere can also act as surfaces for heterogeneous reactions which can lead to ozone destruction and therefore affect the radiative balance (Hofmann and Solomon, 1989;LeGrande et al., 2016).

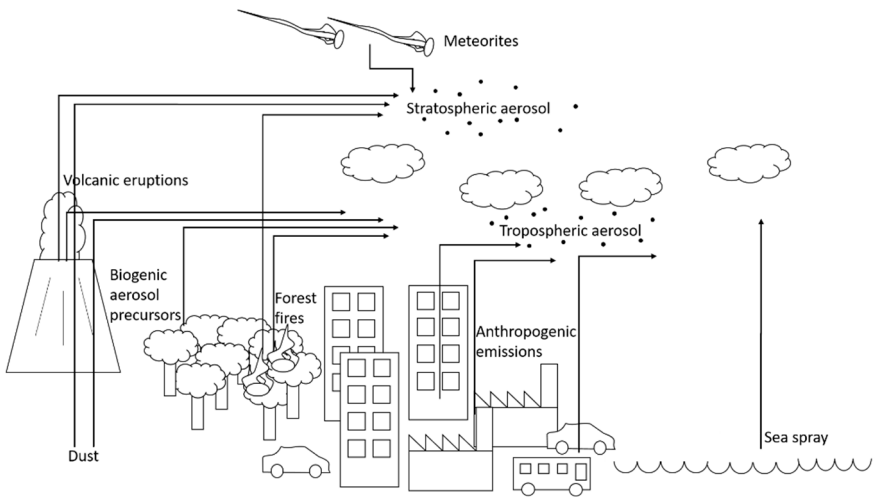

Figure 1
Sources of aerosols.

Primary and secondary aerosols

Aerosol particles directly emitted from a source are called primary aerosols. Examples of these are: Road dust, soot, pollen, sea-salt spray, and volcanic ash. Primary aerosols generally consist of larger particles. This also means that they will have a higher terminal falling velocity and thus remain airborne for shorter times compared to smaller particles.

Aerosol particles can also be formed from molecules condensing onto existing particles in the air or together with each other. Most of these secondary particles are formed by condensation onto pre-existing particles. Examples of these secondary aerosol particles are organic aerosol and volcanic sulphate aerosols. These particles are generally small and can remain suspended in the air for a long time.

Health impact

Inhalation of aerosols can negatively impact health (Lelieveld et al., 2015;Lelieveld et al., 2019). Diseases associated with unhealthy levels of aerosols are various cardiovascular diseases, asthma and several other. Asbestosis is caused by inhaling the long thin asbestos fibres deep into the lungs. Due to their small size, the asbestos fibres can be suspended in the air as aerosol particles. Around 3 million premature deaths occur each year because of the health effect from ambient aerosols (Watts et al., 2020). Episodes of especially unhealthy levels of air pollution is also dependent on the local meteorology (Hou and Wu, 2016), and a meteorological temperature inversion (hot air above colder air near the surface) can effectively put a lid over a city. The result is a build-up of rising levels of air pollution. Human direct contact with sulphur dioxide can be damaging for the respiratory system and cause eye irritation (https://www.who.int/en/news-room/fact-sheets/detail/ambient-(outdoor)-air-quality-and-health). The stratospheric sulphur in this thesis does not have a health effect and have been studied from afar with satellites and aircraft.

Sources to stratospheric aerosols

Background

In the stratosphere there is a background aerosol layer. This is made up from sulphate particles, organic carbon particles, and extra-terrestrial particles from meteors. More than half of the background sulphate particles is likely formed from carbonyl sulphide

(OCS) (Sheng et al., 2015). The major sources for OCS are the oceans and anthropogenic sources (Watts, 2000). This OCS is not broken down in the troposphere since it needs to be illuminated by UV-light. Thus, OCS rises in the tropics, through the so called tropical transition layer (TTL), to altitudes above the ozone layer and then break down and form sulphate particles (Kremser et al., 2016). Altitudes of roughly 30 km can be seen as a ceiling for the sulphate aerosol, as the temperature in the stratosphere increases with height and eventually evaporates the sulphate particles (Kremser et al., 2016). The sulphate particles are small, with radii less than 0.2 μm, and therefore slowly fall down to the lower levels of the stratosphere (Stratosphere-troposphere Processes and their Role in Climate (SPARC), 2006;Kremser et al., 2016). The number concentration of stratospheric aerosol particles peaks at around 20 km altitude (Deshler, 2008).

It has been found that the stratospheric aerosol also contains particles with the elemental signature characteristic of the elements found in meteors (Murphy et al., 1998). This means that as the meteors burns up upon entry into the atmosphere they leave small particles that remains in the stratosphere.

Stratospheric aerosol particles also contain carbon, mostly as organic carbon but also as black carbon (soot and other incomplete combustion leftovers) (Friberg et al., 2014). The amount and type of carbon content makes the particles have varied optical properties. If there is more black carbon in the particles, then more light is absorbed and less is scattered. When radiation is absorbed, the particle is heated and can rise to higher altitudes or evaporate water. If there is more organic carbon compared to black carbon, then more light is backscattered. Since organic carbon is complex, the density and refractive index can vary. Higher organic density and refractive index would lower and increase the scattering of light respectively.

Counterintuitively, the background stratospheric aerosol is also made up by variable and periodic sources. Part of these sources are frequent moderate volcanic eruptions whose emissions also enter the stratosphere. Hydrogen sulphide (H_2S) emitted from volcanoes can also form stratospheric sulphate aerosol, albeit in smaller quantities than from volcanic SO_2 (Kremser et al., 2016). Large wildfires also contribute to the background aerosol. During the Asian monsoon, particles are lifted right up to the border between the troposphere and the stratosphere. Some of these particles are then transported further into the stratosphere. In paper II, the formation of aerosol in the lower stratosphere was studied and shown that it is a complex process with a significant organic component.

Volcanic

When you see a volcanic plume what you are looking at is actually made out of tiny ash pieces of volcanic rock being blown upwards. Unless there was vegetation around the volcanic crater there is very little actual smoke in the plume. Even though the ash particles are small, they fall down quite rapidly compared to the transport of gases that are also emitted in an eruption.

The most emitted gases are H_2O, CO_2 and SO_2. All three have effects on our environment. H_2O and CO_2 are well known for the greenhouse effect but since there are so many other sources for these gases on our planet and water is cycled quickly the emission of these from volcanic eruptions are relatively tiny. Volcanic SO_2 on the other hand is a massive source compared to other sources of stratospheric SO_2 and the resulting aerosol can have a climate impact (Deshler, 2008;Kremser et al., 2016). The biggest volcanic emissions of SO_2 between the years 2000 and 2015 are presented in Table 1, with most of them being covered by the papers in this thesis. Halogenic gases, such as HCl, can also be released and affect high altitude ozone levels.

When SO_2 comes into contact with OH-radicals in the stratosphere it is oxidized into H_2SO_4. In the gas phase, the SO_2 is oxidised through the follow reaction (Heard et al., 2012):

$$SO_2 + OH + M \rightarrow HSO_3 + M$$

Here M is an ambient air molecule. HSO_3 is then further oxidised into H_2SO_4. The H_2SO_4 and water molecules condenses onto pre-existing particles and grows into spherical droplets. These droplets contain on average 75 % H_2SO_4 and 25 % H_2O, but the exact relationship varies with pressure and humidity of the surrounding air.

If the eruption emission does not reach the tropopause, the eruption will have a short residence time. If the eruption emission instead crosses the tropopause, it can traverse the globe in the matter of only two weeks.

Table 1
The biggest volcanic eruptions and forest fires from 2000 to 2015. Table is from Friberg et al. (2018).

Volcano	Date	Lat.	Long.	VEI[a]	SO_2 (Tg)
Ulawun	29 September 2000	5°S	151°E	4	NA
Shiveluch	22 May 2001	57°N	161°E	4	NA
Ruang	25 September 2002	2°N	125°E	4	0.03[b]
Reventador	3 November 2002	0°S	78°W	4	0.07[b]
Anatahan	10 May 2003	16°N	146°E	3	0.03[b]
Manam	27 January 2005	4°S	145°E	4	0.09[b]
Sierra Negra	22 October 2005	1°S	91°W	3	NA
Soufrière Hills	20 May 2006	17°N	62°W	3	0.2[c]
Rabaul Rb	7 October 2006	4°S	152°E	4	0.2[b]
Jebel at Tair	30 September 2007	16°N	42°E	3	0.08[d]
Great Divides Fire Gd	1 December 2006	37°S	144°E	–	–
Chaitén	2 May 2008	43°S	73°W	4	0.01[e]
Okmok	12 July 2008	53°N	168°W	4	0.1[d]
Kasatochi Ka	7 August 2008	52°N	176°W	4	1.7[d]
Fire in Victoria Vi	7 February 2009	37°S	145°E	–	–
Redoubt	23 March 2009	60°N	153°W	3	0.01[f]
Sarychev Sa	12 June 2009	48°N	153°E	4	1.2[g]
Eyjafjallajökull	14 April 2010	64°N	20°W	4	NA
Merapi Me	5 November 2010	8°S	110°E	4	0.4[h]
Grimsvötn Gr	21 May 2011	64°N	17°W	4	0.4[i]
Puyehue Cordón Caulle Pu	6 June 2011	41°S	72°W	5	0.3[i]
Nabro Na	12 June 2011	13°N	42°E	4	1.5[i]
Kelut Ke	13 February 2014	8°S	112°E	4	0.2[j]
Calbuco Ca	23 April 2015	41°S	73°W	4	0.3[k]

[a] Volcanic Explosivity Index (from Global Volcanism Program, http://www.volcano.si.edu/, last access: 14 November 2017).
[b] Prata and Bernardo (2007). [c] Carn and Prata (2010). [d] Thomas et al. (2011). [e] Carn et al. (2009). [f] Lopez et al. (2013).
[g] Haywood et al. (2010). [h] Surono et al. (2012). [i] Clarisse et al. (2012). [j] Li et al. (2017). [k] Pardini et al. (2017).

Forest fires

Massive forest fires can inject smoke into stratosphere (Bourassa et al., 2019). Just as with volcanic particles, the smoke particles can disperse over large distances. The smoke particles have a high soot content. This means that they absorb more light than other particles which in turn mean that they will be heated by sunlight and rise (de Laat et al., 2012;Khaykin et al., 2018). The sunlight also ages these particles through photochemical aging by vaporizing the longer carbon chains into smaller segments until there is only carbon dioxide left. This process might make these particles more short-lived in the stratosphere compared to volcanic sulphate particles. Examples of forest fires large enough to bring smoke into the stratosphere are the fires in western Canada in 2017 and the Australia fires around new Year in 2019/2020. In paper IV, the optical properties of the forest fire smoke are studied and it is explored how they change in early phases of its transport in the stratosphere.

Stratospheric height coordinates

As air in the stratosphere is far above the ground there is a need for height coordinates that are appropriate to describe the air transport and dynamics in addition to the geometric altitude. Air pressure is a height coordinate but several variables are also used to describe the height of the air.

Geometric altitude and geopotential height

Perhaps the simplest height coordinate is geometric altitude, which is commonly defined as the altitude above sea level. Modern commercial aircrafts measure the pressure in the surrounding air and calculate the height above sea level from that. This is possible since atmospheric pressure decreases as the altitude increases:

$$h_{asl} = 44307.69 \times (1 - \left(\frac{p}{p_0}\right)^{0.190284})$$

Where h_{asl} is the geopotential altitude above sea level in meters, p is the pressure and p_0 is the average surface pressure.

Potential vorticity

Potential vorticity is a measure of dynamic stability. Stability means how much the air will be restricted to move about freely. Potential vorticity can thus be used to measure stratospheric circulation (Hoskins, 1991).

A higher potential vorticity usually means that the air originates higher up in the atmosphere. Thus potential vorticity can be used as a height indicator on air parcels as was used later in Fig. 4 and the tropopause can also be described as a surface of constant potential vorticity. Potential vorticity is commonly used as height coordinate for the lowermost part of the stratosphere.

Potential temperature isentropes

When sunlight hits the earth surface, some of it is radiated as heat thus warming the surrounding air. The temperature decreases with altitude in the troposphere and at the tropopause it is at its minimum. Above the tropopause, temperatures start to increase again owing to the oxygen molecules' absorption of UV light and the formation of ozone. As temperatures at different pressures are not ready for comparison, "potential"

temperatures are calculated as the temperature each air parcel would have if they were adiabatically transported down to the earth's surface. The equation for potential temperature is:

$$\theta = T\left(\frac{p_0}{p}\right)^{R/c_p}$$

Where θ is potential temperature, T is the in-situ temperature, p_0 is the reference pressure (set to 1000 hPa), p is the in-situ pressure, R is the gas-constant and c_p is specific heat capacity.

Atmospheric structure

The atmosphere is layered. Each layer has unique features and sometimes the distinction between them is blurred. A simplified view of the lower layers of the atmosphere is shown in Fig. 2. This thesis has focused on the stratosphere, with papers II and III having extra focus on transport between the different layers in the lowermost stratosphere. This is also the region where normal passenger aircraft fly in at extratropical latitudes.

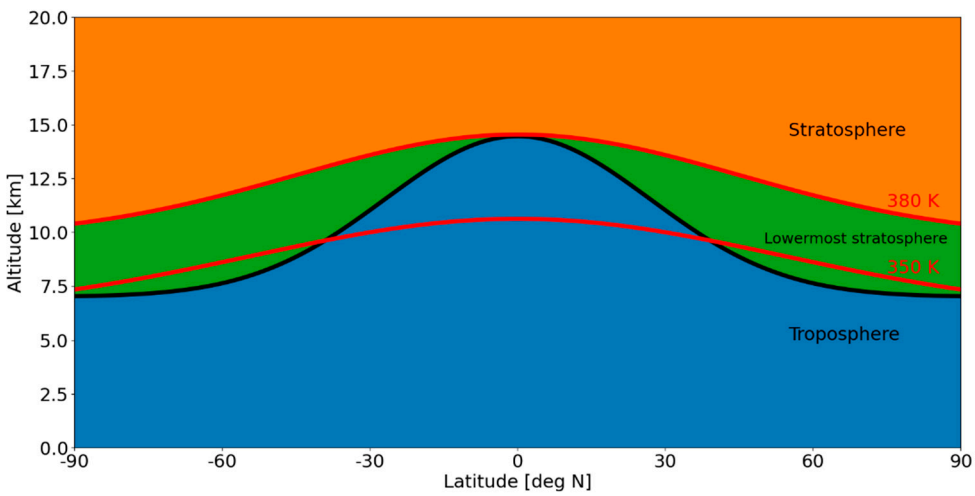

Figure 2
Illustration of the atmospheric structure from the surface to the lower stratosphere. The thick black line indicate the tropopause. The red lines mark surfaces where the potential temperatures are constant. The 380 K line marks the border between the lowermost stratosphere and the rest of the stratosphere. The 350 K isentrope shows that the potential temperature can be constant and still cross the tropopause.

The troposphere is the layer where weather occur and spans from the ground up to the tropopause. The tropopause will be explained in the next section. Since the troposphere has vertical mixing and hosts all kinds of weather, this layer is highly diverse and changes are driven by temperature and pressure differences in the air. Aerosols in this layer have relatively short lifetimes of roughly one week (Jacob, 1999) and are removed by uptake in cloud particles, by rain or by dry deposition.

Tropopause

The tropopause is the upper limit of the troposphere and the lower limit of the stratosphere. The altitude of the tropopause varies with latitude and season but is on average at 8 km altitude at the poles and 18 km altitude at the equator. There are several different methods of defining where the tropopause is. The methods are based on different atmospheric characteristics: Lapse rate, chemical tropopause and potential vorticity.

The lapse rate in the atmosphere is how temperature changes with altitude. The further up in the troposphere the colder it gets but the further up in the stratosphere the warmer it gets, see Fig. 3. Using this information, the border between the troposphere and stratosphere is set to where it stops getting colder, usually where it gets less than 2 K colder per km. As a consequence of this temperature drop, the tropopause is where the coldest temperatures are found. Because the tropopause altitude is higher at latitudes with warmer surface temperature, it is at the tropical tropopause where the atmosphere is the coldest.

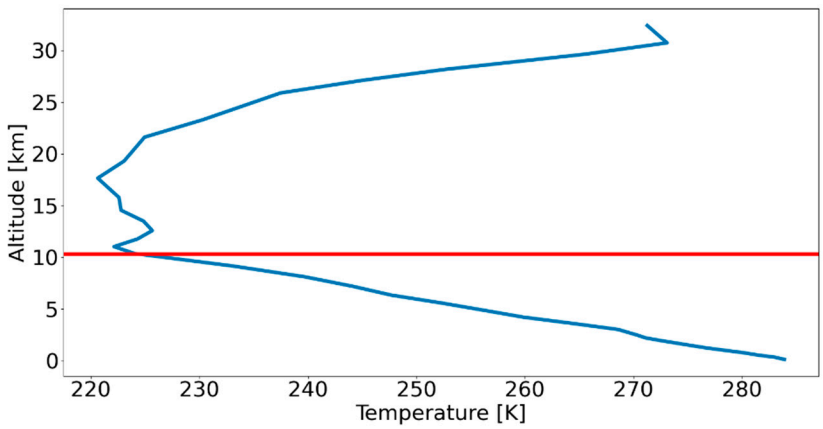

Figure 3
The temperature profile (in blue) over Lund, Sweden on 2009-06-19. The lapse rate tropopause is indicated by the red horisontal line. Temperature data is from the ERA5 dataset (Hersbach et al., 2020).

The troposphere and stratosphere are different also from a chemical point of view. The stratosphere contains the ozone layer and is therefore rich in ozone. This is not the case for the troposphere where the ozone levels are significantly lower and ozone containing smog is limited to fairly low altitudes. The troposphere contains trace amounts of CO from all surface activities. Apart from aircraft emissions and the occasional smoke from massive forest fires, there aren't many sources for CO in the stratosphere. By measuring these two chemical molecules' concentrations with altitude, one can see where ozone becomes more dominant than CO. This is called the chemical tropopause.

There is also a variable called the potential vorticity, that one can calculate for air parcels. Potential vorticity is a measure of the dynamical stability a parcel of air has and is a conserved quantity when the air parcel is moved adiabatically in the atmosphere. It has its own unit, the potential vorticity unit or PVU for short, where 1 PVU = 10^{-6} K m^2 kg^{-1} s^{-1}. The potential vorticity of air in the stratosphere is higher and the tropopause is often defined as when a threshold in potential vorticity is crossed. The limit is usually set between 1.5 to 3.5 PVU. In papers I, II and III, the limit 1.5 PVU has been used since it captures all air parcels with hints of the stratosphere. At the tropopause, a change of 1.0 PVU is roughly equal to a change of 0.5 km altitude. There, one can divide the stratosphere into even thinner layers, see Fig. 4.

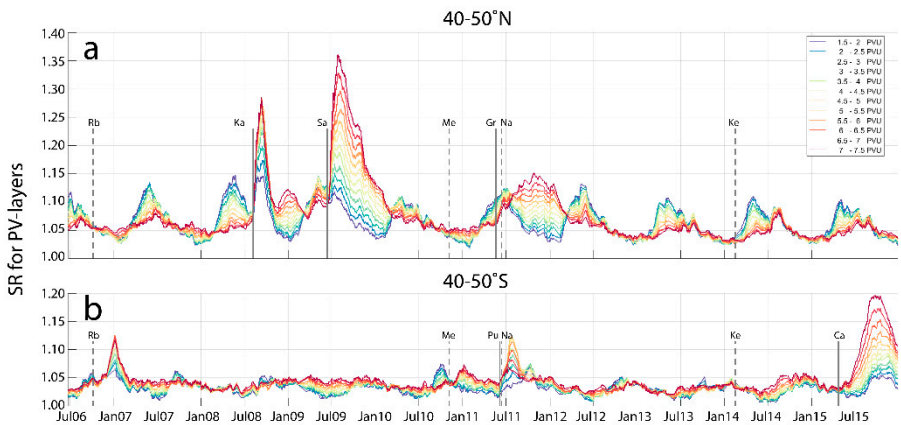

Figure 4
The scattering from aerosol particles in many subdivided layers of the stratosphere, where 1 PVU is roughly 500 m. See Table 1 for the abreviations of the volcanic eruptions. This was used in paper I instead of the more traditional and coarser subdivision of the stratosphere to show that downward transported volcanic aerosol reached 1.5 PVU and that there are less and less tropospheric sources for the stratospheric aersol from the tropopause and above. This figure is from Friberg et al. (2018).

Stratosphere

The stratosphere is situated from the tropopause to the stratopause, the border to the next layer (the mesosphere) which is roughly at 50 km. The extreme cold temperatures at the tropopause dries air that enters the stratosphere from below. This drying leads to almost a complete absence of meteorological clouds in the stratosphere. Therefore, particles from volcanic eruptions increase the scattering of light compared to the background aerosol.

If small particles reach the stratosphere they will remain here for a long time since gravity pulls small particles with less force. Particles can also be removed due to vaporization due to the higher temperatures at increasing altitudes in the stratosphere. The stratosphere hosts the ozone layer but also a layer of sulphate particles, called the Junge layer.

Lowermost Stratosphere

The lowermost stratosphere (LMS) is defined between the local tropopause altitudes and the 380 K isentrope surface (Hoor et al., 2005). This region has some exchange with the troposphere (Lelieveld et al., 1997). Since the LMS is located at fairly low altitudes, it was previously overlooked in global climate simulations. But it has been discovered that particles in this lowest stratospheric layer have an effect on the climate as significant amounts of volcanic aerosol particles can remain there for long periods of time (Andersson et al., 2015). Satellite and in-situ aircraft measurements of the LMS aerosol were compared in paper III.

Since the LMS is bordered by the troposphere and the overlying stratosphere, gradients of gas and particle concentrations show gradual transitions in this part of the stratosphere. In the extra-tropics there is bi-directional transport across the tropopause, which means that the gradients of trace gases typically used to define the transition from the troposphere to the stratosphere are less pronounced. Therefore, this layer around the tropopause at these latitudes has been named the extra-tropical transition layer (ExTL) (Gettelman et al., 2011).

Stratospheric dynamics

Brewer Dobson circulation

As air rises in the hot tropics it will eventually reach the tropopause and cross it (Appenzeller et al., 1996). If it crosses it there will be two transport cases. One is above the tropopause in the direction toward the nearest pole and gradually loses altitude. The second option is for the air to continue further up and then spread towards the poles. As expected, the shallow option requires less time than the deep case of upward transport. Both cases are parts of the Brewer Dobson circulation (Butchart, 2014). The Brewer-Dobson circulation is illustrated in Fig. 5. In general, aerosol and aerosol precursors entering the stratosphere in the tropics are transported out of the stratosphere at more poleward latitudes.

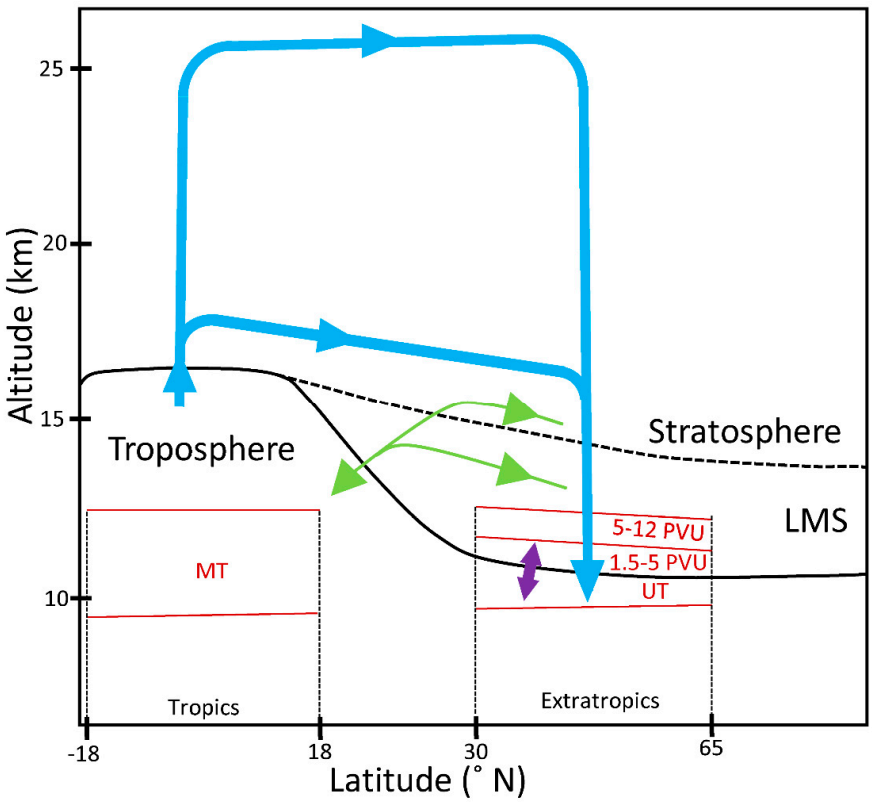

Figure 5
The Brewer-Dobson circulation shown with blue arrows. During summer, the barriers between troposphere and stratosphere is weakened in the subtropics. The resulting transport is shown by the green arrows. The purple arrow indicate cross-tropopause transport. This figure is from paper II.

If an explosive volcanic eruption occurs in the tropics, then the aerosol can be transported upwards in the upper branch of the Brewer Dobson circulation or towards the poles in the lower branch of the Brewer Dobson circulation. If an eruption occurs closer to the poles and just reaches the LMS, then the aerosol is unlikely to reach the other hemisphere and will be pushed down into the troposphere by the Brewer Dobson circulation. It is understandable that the aerosol from a tropical eruption will stay in the stratosphere longer than the aerosol from an eruption closer to the poles.

Measured sulphur in aerosol sample can be a tracer of the Brewer-Dobson circulation (Diallo et al., 2017). If one measures a high sulphur concentration at background conditions in the LMS, then it is likely that the air has been transported through the deep branch. If the background concentrations are low, then it is likely that the air is more local or transported through the shallow branch.

Isentropic transport

Without external power, aerosol particles will remain at constant potential temperature. The aerosol particles will therefore be transported on surfaces of potential temperatures. These surfaces are not aligned with geometric altitudes. The 380 K isentrope defines the upper limit of the LMS which coincides with the tropopause in the tropic. None of the isentropes in the troposphere reaches the stratosphere above the LMS. Therefore, transport along constant potential temperatures allows for transport across boundaries between the troposphere and the LMS. This is shown in Fig. 5 with the green arrows.

Asian Tropopause Aerosol Layer (ATAL)

During the Asian monsoon in summer months, air is also lifted upwards. The air brings a lot of particles with it and creates a layer of them around the tropopause. This yearly phenomenon is called the Asian Tropopause Aerosol Layer, or ATAL for short, and is a quite recent discovery (Vernier et al., 2011;Vernier et al., 2015;Yu et al., 2015). ATAL covers quite a large region and it is contained inside 15-45°N, 15-105°E. There were no observations of it before 1999 (Thomason and Vernier, 2013). The effect of ATAL was likely present in both paper II and III as a source of uncertainty but the effect is small compared to that of volcanism. There is still some uncertainty of what it is made up of chemically and research is on-going to accurately measure it (Vernier et al., 2018).

Subtropical jet

Fast stratospheric winds encircling the poles north of the tropics block transport from the tropical troposphere to the LMS (Haynes and Shuckburgh, 2000) and these winds are called the subtropical jet. During summer these winds are weakened, allowing for transport of the ATAL into the LMS. The weakening of the winds is coincident with Rossby Wave Breaking (RWB), which looks like waves on horizontal maps at 350 K altitude. In both papers II and III, the subtropical jet was important for explaining the transport mechanism of the aerosol.

Methods

Remote sensing

When volcanoes erupt in remote places, satellites are indispensable tools for measuring them accurately. This has been done for several decades with the satellite instruments increasing in resolution and in their sophistication.

By flying many satellites carrying different instruments after each other in the same track, their data can be combined to provide unique views of the atmosphere. Currently the satellites in the so called Afternoon-train are (in flight order): OCO-2, GCOM-W1, Aqua, CALIPSO, CloudSat and Aura. The name, Afternoon-train, comes from that the satellites pass over the equator in the afternoon.

CALIOP

By sending out light from a laser against aerosol particles and then detecting the backscattered light, several things are measured: The amount of backscattering done by the target is measured through the intensity of the returned signal. The distance between the lidar and the target is measured by timing the light from emission of the pulsed laser and the measurement of the backscattered signal. Advanced lidar systems send out light in several different wavelengths and are polarization sensitive. By using data from multiple wavelengths, particle size can be investigated.

The equation that explains the power of the light returned to the lidar system is called the lidar equation and is written as:

$$P(r) = P_0 \eta \left(\frac{A}{r^2}\right) O(r) \left(\frac{ct}{2}\right) \beta(r) \exp\left[-2 \int_0^r \alpha(r')\mathrm{d}r'\right]$$

Where $P(r)$ is the power received by the lidar at range r, P_0 is the emitted power of the beam, A is the area of the detector, $O(r)$ is the overlap function (which tells how much of the studied height interval is "seen" by both the emitter and detector), c is the speed of light, t is the duration time of the laser pulse, $\beta(r)$ is the light backscattering and $\alpha(r')$

is the light extinction at a point between the lidar and target. The exponential in the equation describes how the signal is attenuated to and from the aerosol particle, and is commonly referred to as the two-way transmission factor.

Aerosol optical depth (AOD) is a measure of how much the aerosol blocks incoming light. The AOD is calculated by integrating the aerosol extinction coefficients over height. If aerosol extinction coefficients were not directly measured by the lidar system, then they can in turn be calculated by multiplying the aerosol backscattering with a variable called lidar ratio which is dependent on the type of aerosol.

CALIPSO (Cloud-Aerosol Lidar and Infrared Pathfinder Satellite Observation) is a polar orbiting satellite. One of CALIPSO's payloads is CALIOP (Cloud-Aerosol Lidar with Orthogonal Polarization) which is a polarization sensitive lidar (Winker et al., 2009). The CALIOP lidar sends out a laser beam which is then scattered by aerosols and air in the atmosphere. By measuring the time taken for the scattered laser beam to return to the satellite one can calculate the altitude of the aerosol with a resolution up to 30 m. This highest resolution is available for altitudes below 8 km. Between 8 and 20 km the resolution is 60 m and between 20 and 30 km the resolution is 180 m. Depending on the shape of the aerosol the polarization can be changed or remain the same. Sulphuric aerosol from volcanic eruptions contain H_2SO_4 and H_2O in the form of spherical droplets which can be detected with CALIOP (Vernier et al., 2009;Andersson et al., 2015;Friberg et al., 2018;Sandvik et al., 2019). Spherical particles do not change the polarization of the laser beam. Soil dust, volcanic ash, and ice particles have very irregular shapes. Particles with irregular shapes change the polarization of the laser beam. Thus, by measuring polarization the particle type can be investigated (Prata et al., 2017).

The footprint of CALIOP when the laser beam arrives at the surface is around 70 m. However, as the backscatter signal gets weaker higher up in the atmosphere and the signal to noise ratio is worse, the signal needs to be averaged. This means that the horizontal resolution ranges from 333 m to 5000 m. Between 8.5 km and 20.1 km altitude the horizontal resolution is 1000 m. The high resolution of a CALIOP swath is evident in Fig. 6, where an example swath is visualized. This swath was taken shortly after the 2009 Sarychev eruption and contains stratospheric volcanic aerosols. Note also how potential temperature increase with altitude. Regular temperature on the other hand decreases with altitude up to the tropopause and then starts to increase.

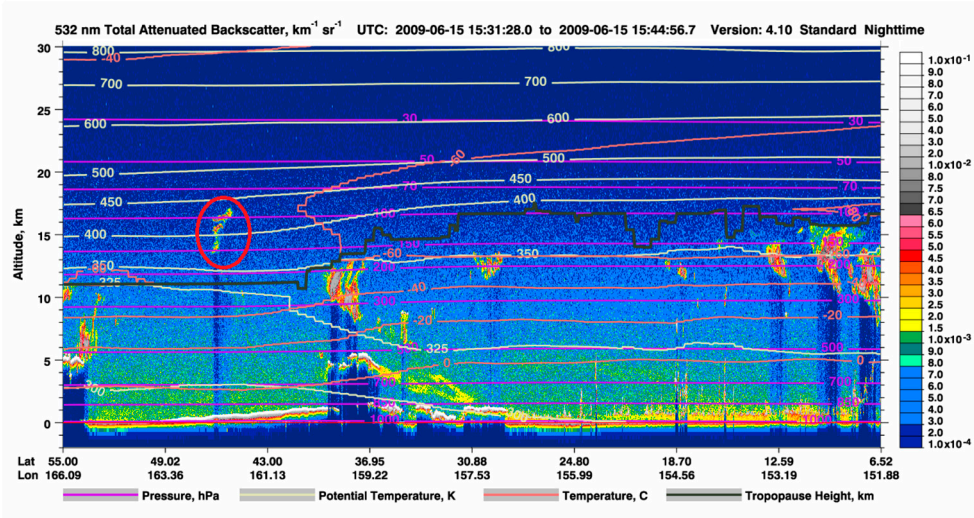

Figure 6
A CALIOP swath of backscattering data. This swath also contains aerosol from the Sarychev 2009 eruption, as is highlighted in the red circle. This figure is part of the CALIOP browse images from NASA.

During the satellite's lifetime, several operational changes has affected the subsequent data products. Due to problems with reflection from horizontally oriented ice particles, the nadir (downward-looking) angle was changed from 0.3° to 3° in year 2007. In 2018, CALIPSO lowered its orbit from 705 km to 688 km so that it would fly in formation with CloudSat.

CALIOP measures both during night and day. Daytime measurements are noisier since solar light can be reflected towards the satellite and cause interference with the lidar signal. Around the eastern part of South America, the South Atlantic anomaly (SAA) disturbs the CALIOP signal and increases noise levels. The CALIOP data is calibrated by using aerosol-free measurements at high altitudes (Kar et al., 2018).

In the most basic product, CALIOP measures the total attenuated backscattering which has the unit of km^{-1} sr^{-1}, where sr stands for steradian (also known as solid angle). The aerosol specific measurements aerosol backscattering and scattering ratio were calculated from the CALIOP data. The aerosol backscattering was calculated by subtracting molecular backscattering from the total backscattering. Similarly, scattering ratio was calculated by dividing the total backscattering with the molecular backscattering. The molecular backscattering was calculated for a given CALIOP pixel using the supporting meteorological data that comes with the data product. In a homogeneous column of air, aerosol backscattering becomes smaller with increasing altitude (lower pressure) due to the air getting thinner. Scattering ratio, on the other

hand, remains the same as it is the fraction of scattering that comes from aerosol particles in an air parcel compared with the scattering from both aerosol and the background air molecules.

The data from CALIPSO were used for papers I, III, IV and V in this thesis. For each paper the data analysis differed slightly. For the papers focused on long timespans (papers I and III), the data from CALIOP swaths were averaged over time, whereas for papers focused on specific events (papers IV and V) used individual swaths. To select the stratospheric aerosol in CALIOP swaths, the tropopause needs to be defined. In the CALIOP data product, heights for the thermal tropopause are supplied. These tropopause heights were used in papers IV and V. As to not miss air masses with stratospheric characteristic but which were residing below the thermal tropopause, another tropopause based on levels of potential vorticity was used in papers I and III.

Once the stratospheric part of the CALIOP data has been selected, the aerosol need to be classified as either background, ice-clouds, polar stratospheric clouds, smoke or volcanic. As ice-cloud particles are depolarizing, depolarization ratios calculated from the CALIOP data were used in all papers to classify data as ice-clouds. At high latitudes, polar stratospheric clouds are located high up and were classified based on temperature in paper I. This was the only paper which studied areas where polar stratospheric cloud resides. When individual swaths were studied in papers IV and V and the aerosol layers were observed shortly after they appeared in the stratosphere, the observed scattering was also used to separate the background from the pixels containing smoke and volcanic aerosol.

In paper I, the CALIOP data were averaged into 1° × 1° latitude boxes. Thresholds for potential vorticity and depolarisation ratio were used to select the stratospheric aerosol studied in papers I-III. In paper V, CALIOP swaths containing volcanic stratospheric aerosol were found by manual inspection together with cross-correlating with SO_2 observations from other satellites and the thermal tropopause supplied with the CALIOP product was used to define the tropopause. Right after an eruption, the volcanic aerosol is transported as dense cloud-like formations with clearly elevated values of scattering ratio. In paper V, when early volcanic aerosol layers from the 2009 Sarychev eruption were used, the surrounding background in the swath was filtered away using thresholds for scattering ratio.

CALIOP's lidar beam has two wavelengths, 532 and 1064 nm. The ratio between the scattering of the long wavelength with that of the shorter is called the colour ratio. The colour ratio is sensitive to the size of the probed aerosol particles. Colour ratio was used in paper IV to investigate if the size of aerosol particles from forest fires changed and in paper V when manually inspecting swaths for ice clouds.

AIRS

Atmospheric Infrared Sounder (AIRS) is as the name suggest an infra-red sounder. What this means is that it measures in the infra-red range what is emitted from the atmosphere. Different chemical elements absorb different amounts of the signal in different wavelengths. This makes it possible to calculate the chemical composition of the atmosphere based on the signal. SO_2 is one of these chemical elements that can be determined (Prata and Bernardo, 2007;Prata et al., 2010;Thomas et al., 2011).

SO_2 has absorption bands in the ultra-violet and infrared parts of the spectrum. For the infrared part there are three distinct absorption peaks at different wavenumbers: 1152 cm^{-1}, 518 cm^{-1}, 1362 cm^{-1} referenced as ν_1, ν_2 and ν_3 bands respectively (Sumpf, 2001;Prata et al., 2010). Measurements at the ν_1 and ν_3 bands are often used to determine atmospheric SO_2 levels since they don't get saturated as quickly as other wavenumbers and there are fewer absorption peaks from other gases at these wavenumbers. The ν_2 band is less of interest since it is difficult to make experimental techniques for this band and the band also has less intensity. The HITRAN database contains spectroscopic data for many molecules (Gordon et al., 2017). In paper V, SO_2 column densities from AIRS were used.

The physical explanation for why the absorption peaks occur at the ν_1 and ν_3 bands are that at the ν_1 band there is a symmetric stretch mode of the SO_2 molecule and the ν_3 band corresponds to where the asymmetric stretch mode is. A stretch mode is one of the vibrational frequencies of the molecule, the musical equivalent is the frequency of a tuning fork. Absorption at the ν_3 band is much more pronounced than at the ν_1 band. When absorption at both ν_1 and ν_3 bands happens at the same time there is absorption in a region around the sum of the wavenumbers at 2514 cm^{-1}, which can also be seen in spectra. This absorption is weaker since it is rarer but can be used when there are extremely high SO_2 concentrations.

Since AIRS uses infra-red wavelengths it can provide data during both day and night. In order to calculate the SO_2 content, other parameters are needed. One of these is the altitude of the SO_2 cloud. In paper V, I produced vertical distributions of SO_2 in AIRS swaths that contained SO_2 from a volcanic eruption. The CALIOP observations were transported with a trajectory model to the time and place of AIRS swaths.

The SO_2 data in paper V were produced by the same method as in Prata and Bernardo (2007). Their method for determining the amount of SO_2 in a pixel is the following: Find the pixel whose spectra is most correlated with background conditions of SO_2. With this background pixel, the contribution from background can be removed in the original pixel. In the original pixel, there will now only be signal from the additional

SO_2 left. This signal can now be compared with synthetic spectra for various levels of SO_2 at different altitudes. The synthetic spectra of a SO_2 level that matches signal with the highest correlation is chosen as the optimal estimate of the SO_2 vertical column density.

OMI

Just as in the infra-red spectrum, the UV spectrum also have distinct absorption peaks for SO_2. The Ozone Monitoring Instrument (OMI) was launched aboard the Aura satellite in 2004. It measures spectrum in the UV and visible wavelengths with a CCD. OMI has high spectral resolution. The measurements are done in a nadir-viewing orientation. This combined with a wide field of view make it possible to observe large areas each swath. The light measured is backscattered sunlight which means that measurements are restricted to daytime swaths.

The OMI instrument has a very high sensitivity for detecting SO_2 and observes among other sources the SO_2 released by volcanoes (Lee et al., 2009;Thomas et al., 2011;Theys et al., 2013;Ge et al., 2016;Carn, 2016;Fioletov et al., 2017). I have used OMI in my work to get an overview of how SO_2 from volcanoes have been transported.

In-situ observations

IAGOS-CARIBIC

The IAGOS-CARIBIC project (In-service Aircraft for a Global Observing System – Civil Aircraft for Regular Investigation of the atmosphere Based on an Instrument Container) measures the atmosphere at altitudes mostly between 9-12 km. It consists of a large number of instruments for atmospheric measurements that are flown aboard a commercial aircraft (Brenninkmeijer et al., 2007). The instruments are fitted in a container which is loaded onto a commercial long distance aircraft once every month. The aircraft is fitted with a custom air inlet which connects to the instrument container so that the sampled air is led to each instrument.

The IAGOS-CARIBIC project has been collecting measurements for more than two decades now. Some of the many flights that has been done with IAGOS-CARIBIC is shown in Fig. 7. Today the project is in the process of being moved to a new aircraft, as the current aircraft will be retired. This new aircraft will be the third aircraft to fly the IAGOS-CARIBIC project.

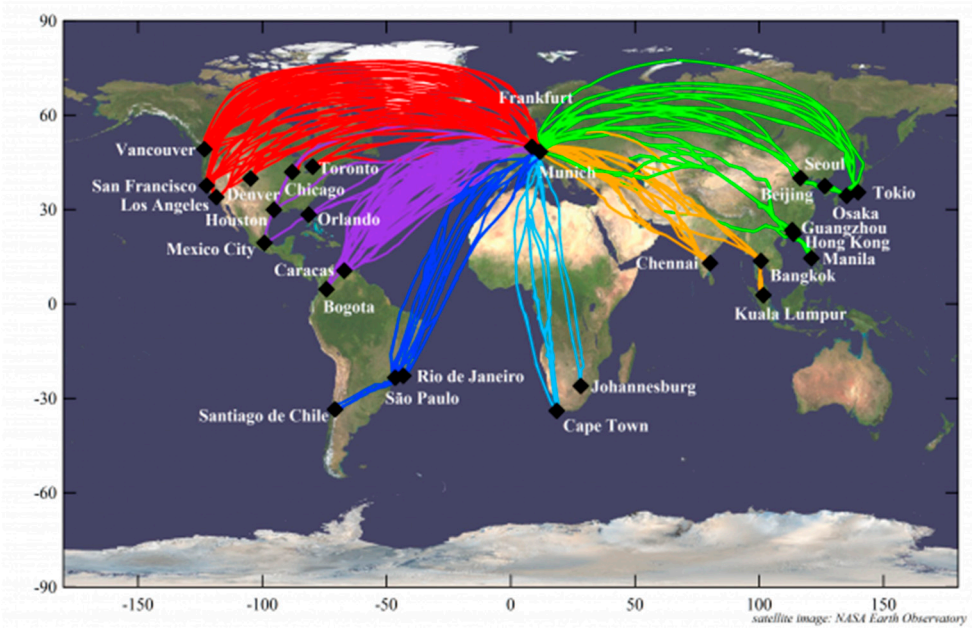

Figure 7
Map of where IAGOS-CARIBIC has collected measurements, from: http://www.caribic-atmospheric.com/ .

One of the many instruments in the container is an aerosol sampler which collects aerosols on 180 nm thin Polyamide films (Papaspiropoulos et al., 1999;Martinsson et al., 2005;Nguyen et al., 2006). The films have been analysed at the Lund Ion Beam Analysis Facility using the methods particle-induced X-ray emission (PIXE) and particle elastic scattering analysis (PESA) to measure the chemical composition.

The PIXE and PESA method consist of irradiating the aerosol samples with a proton beam and observing emitted X-rays and scattered proton. The PIXE method uses the X-rays to identify elements with atomic number larger than 15, whereas the PESA method uses elastically scattered protons and is used for lighter elements. Together the two methods complement each other and provides highly accurate elemental concentration which can detect very low concentrations (Martinsson et al., 2014).

On IAGOS-CARIBIC there is an instrument capable of measuring the number of particles in several size bins. It is called optical particle size spectrometer (OPSS) (Hermann et al., 2016). This instrument makes it possible to observe the size distribution of the aerosol for particles with diameter between 0.1 and 1 µm.

Elemental concentrations obtained from the IAGOS-CARIBIC platform were used in papers II and III. In paper III, aerosol scattering was calculated based on the aerosol

properties measured by IAGOS-CARIBIC. This aerosol scattering was then compared with what CALIOP measured. In paper III, when the sample size was small for some data categories, Student-t distributions were used to find the probable intervals for the underlying normal distribution observed in the IAGOS-CARIBIC data. In order to get a measure of the uncertainty of averaged values, standard errors were also calculated.

Meteorological reanalysis

The European Centre for Medium Range Weather Forecasts (ECMWF) produces meteorological reanalysis products. In paper III, I used the ERA (ECMWF Re-Analysis) Interim product. Reanalysis models are similar to a weather forecast models, but also uses data collected after a studied time.

The newest ECMWF reanalysis product is called ERA5 (Hersbach et al., 2020). It succeeds ERA-Interim and has a finer resolution in the horizontal, vertical and time. Currently, there are longer ques for access since it is quite newly released and many organizations want to download the data. It uses more databases and more satellite data for reanalysis and currently provides data from 1979 to the present. This new ERA5 product was used in paper V.

FLEXPART

The FLEXible PARTicle dispersion model (FLEXPART) is a particle trajectory model that simulates individual computational particles (Stohl et al., 2005;Pisso et al., 2019). By keeping track of each particle's position instead of the particle concentration in a box, the model is called "Lagrangian".

These computational particles are not equivalent to aerosol particles; instead, a computational particle represent an air parcel which can consist of different gases or aerosol particles. Therefore, FLEXPART is used by many researchers for different purposes (Mattis et al., 2010;Kristiansen et al., 2010;Kristiansen et al., 2015;Zhu et al., 2020).

FLEXPART can run both forward and backward simulations. For forward runs, particles are released with a specified mass and the output is presented as concentrations. For backward runs, particles are released and the output is sensitivities. These sensitivities can be seen as likelihoods that the particles originate from a specific area and the unit is seconds. A personal computer is sufficient to run FLEXPART but

the model is also used on supercomputers. In this thesis FLEXPART was run on a personal computer using a Linux environment installed inside Windows 10. FLEXPART also has good support for parallel computing since each particle is effectively run independent from the other particles.

The following ingredients are needed for a successful run:

- Meteorology data prepared for input to FLEXPART.

- A file specifying where particles are released (RELEASES-file). 4D boxes with the number and mass of particles distributed inside it.

- Options that command the overall run. (COMMAND-file). This file sets how long the model should run. I have tried two alternatives: Running the model both backwards and forward in either that each run should last *X* number of days or that each run should be inside a time interval.

- A grid to place the output on (OUTGRID-file).

The final results are averaged and put on a four dimensional grid specified by the OUTGRID-file, with time, longitude, latitudes and altitude being the dimensions. Output resolution is user specified but the accuracy is effectively limited by the resolution of the meteorological data. One needs to consider that high resolution meteorological data will take up more space and is better for studies in a limited region (e.g. Europe). Meteorological data can be reanalysis data from ECMWF and I used the ERA5 product.

In paper V, FLEXPART was used as a central part in a novel method to produce vertical distributions for SO_2 observation. This was done by entering aerosol particles observed by CALIOP to be released in FLEXPART. These particles were then transported with FLEXPART to the time and locations of AIRS swath. The transported particles in these locations were then used to create vertical distributions based on the original CALIOP heights to vertically represent the SO_2 seen by AIRS.

Findings

Background aerosol

One of the aims of the thesis was to better characterize the background aerosol in the stratosphere. Models assume that the particles in the background aerosol mainly contain sulphuric acid and water. However, from previous measurements we know that there is an organic component as well that needed to be better understood.

Therefore, the composition of the background stratospheric aerosol was studied by using the measurements from IAGOS-CARIBIC at altitudes between 9 and 12 km above sea level. As previously mentioned, samples taken with IAGOS-CARIBIC can be analysed to give elemental concentrations with very high sensitivity. Because of the many samples taken during more than a decade it is also possible to observe seasonal changes in the various parts of the atmosphere. The carbon concentrations shown in Fig. 8 follow the same pattern as the sulphur concentrations, notably that the carbon concentrations are higher deeper into the stratosphere. This indicates that carbonaceous aerosol are produced in the stratosphere as the maximum carbon concentration in the upper part of the LMS is found during spring when the transport from the above stratosphere peaks. It is therefore important to consider other types of aerosol particles and not only the sulphuric particles in the stratosphere.

During background conditions, the scattering from stratospheric aerosol peaks during spring in the lowest layer of the stratosphere (Fig. 4). It is not only the transport of aerosol particles from above that contribute to this peak. Increased elemental concentrations characteristic of dust particles have been measured by IAGOS-CARIBIC during this season as well (Martinsson et al., 2005). It is linked to increased levels of aerosol scattering in the troposphere during this season and the peaks are more pronounced in the northern hemisphere. This indicates that even more components than sulphate, water, and carbon exist in the lowest stratosphere.

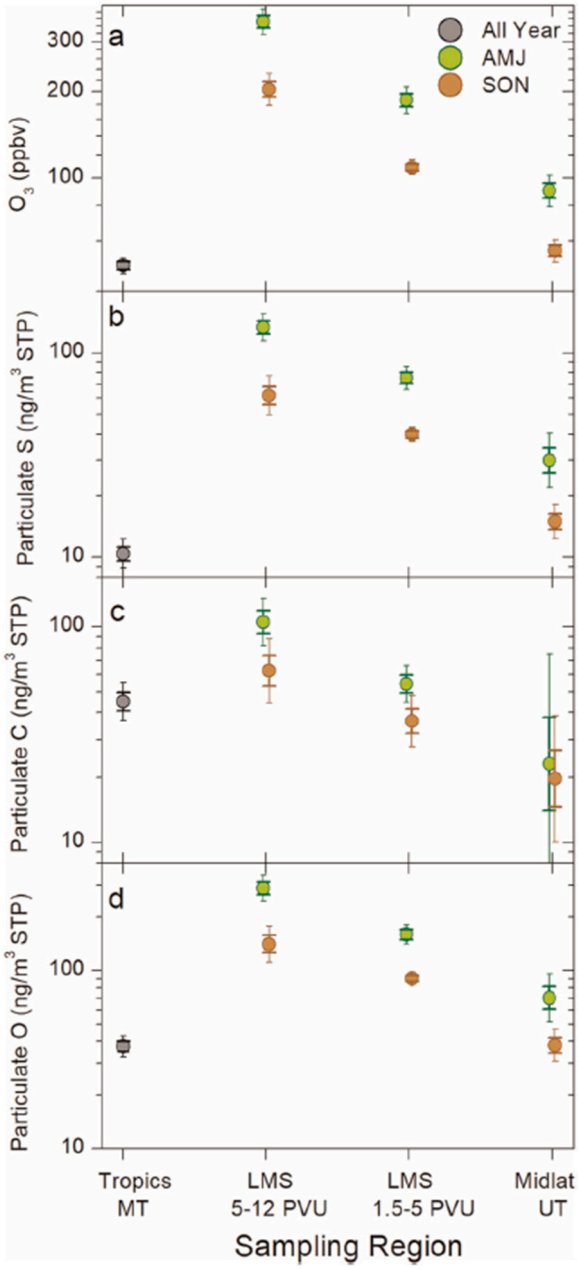

Figure 8
Geometrical averages of measurements made by IAGOS-CARIBIC of O_3 and elemental concentrations of tropospheric and stratospheric aerosol particles. The LMS is divided into two sampling regions based on potential vorticity. As the the aircraft's sampling altitude is usually between 9 and 12 km but the tropopause altitude is different at different latitudes, the upper troposphere has been sampled at midlatitudes and the middle troposphere has been sampled in the tropics. Samples taken in the months April, May and June are labelled as AMJ and the months September, October and November are labelled as SON. This is Fig. 4 in Paper II.

Volcanic aerosol

Volcanic stratospheric aerosol can decrease the surface temperature as they reflect some of the incoming solar radiation. In order for global climate models to be tuned for predicting surface temperature and have correct radiation budgets they need to accurately model the historical climate. To do this successfully, they need data on when large volcanic eruptions have increased the stratospheric aerosol loading among other measurements. If volcanic emission data are unavailable, it could lead to biases in the models. Also, as models have increased resolution, the underlying data products need to improve as well and become more accessible to modellers. This thesis provides a chronology of volcanism's and forest fires' effect on the stratospheric aerosol spanning almost a decade, see Fig. 9. In this figure, the scattering ratio is shown. This figure can be compared to Table 1, as several volcanic eruptions have led to increased aerosol loadings. The largest emissions of SO_2 from volcanic eruptions are also the ones most visible in Fig. 9. The two high-altitude eruptions of Soufrière Hills 2006 and Kelut 2014 gave rise to aerosol that remained at high altitude and mostly stayed in the tropics. The reason for this was that they were entrained by the deep branch of the Brewer-Dobson circulation. If the volcanic aerosol instead would have formed slightly above the LMS or below 20 km in the extratropical or tropical regions, they would have been able to spread across a wider latitude interval. This happen for the aerosol from the tropical eruptions of Rabaul 2006, Merapi 2010 and Nabro 2011. Aerosol formed in the LMS, such as part of the Kasatochi 2008 eruption and the Sarychev 2009 eruption, would eventually be transported down into the troposphere. Note also how the aerosol from extratropical eruptions tend to stay within their original hemisphere. Overall, the volcanic eruptions raised the stratospheric AOD by 40 % on average in the study period.

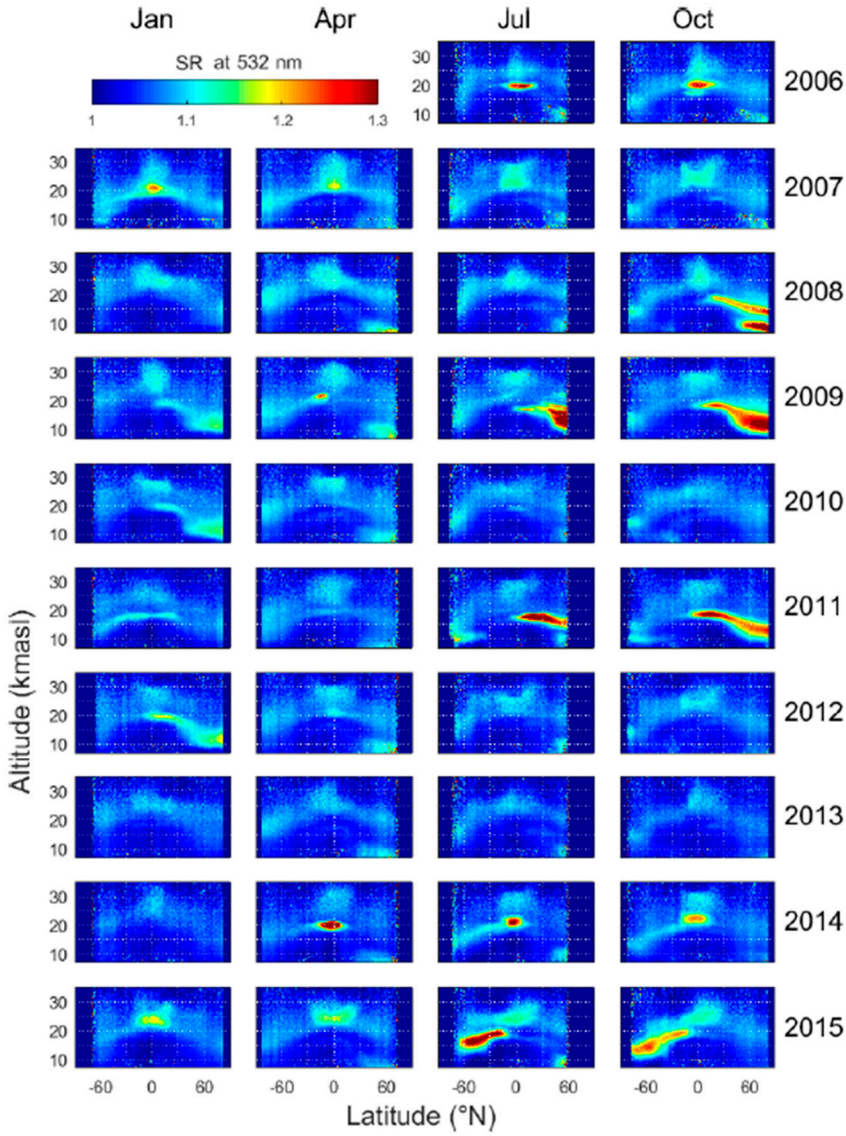

Figure 9
Chronology of the scattering ratio as monthly mean values from the CALIOP instrument. This is Fig. 4 in paper I.

In Fig. 10, the aerosol scattering measured by CALIOP is compared to the calculated aerosol scattering from IAGOS-CARIBIC measurements. These calculations are based on the assumptions that the aerosol consists of sulphuric acid, water and organic carbon. For aerosol particles closer to the tropopause, the calculated scattering from IAGOS-CARIBIC measurements is less than the scattering observed by CALIOP. The aerosol composition is different in the LMS (and particularly in the ExTL) than the overlying stratosphere. This different composition can come from crustal particles and nitrate. Also, particles can grow in size with water. These reasons can help explain the different results by the two measurement platforms. The best agreement between the two measurement platforms was when the sampled air was affected by medium-sized volcanic eruptions, which suggests that the volcanic sulphate aerosol is well represented in the calculated scattering.

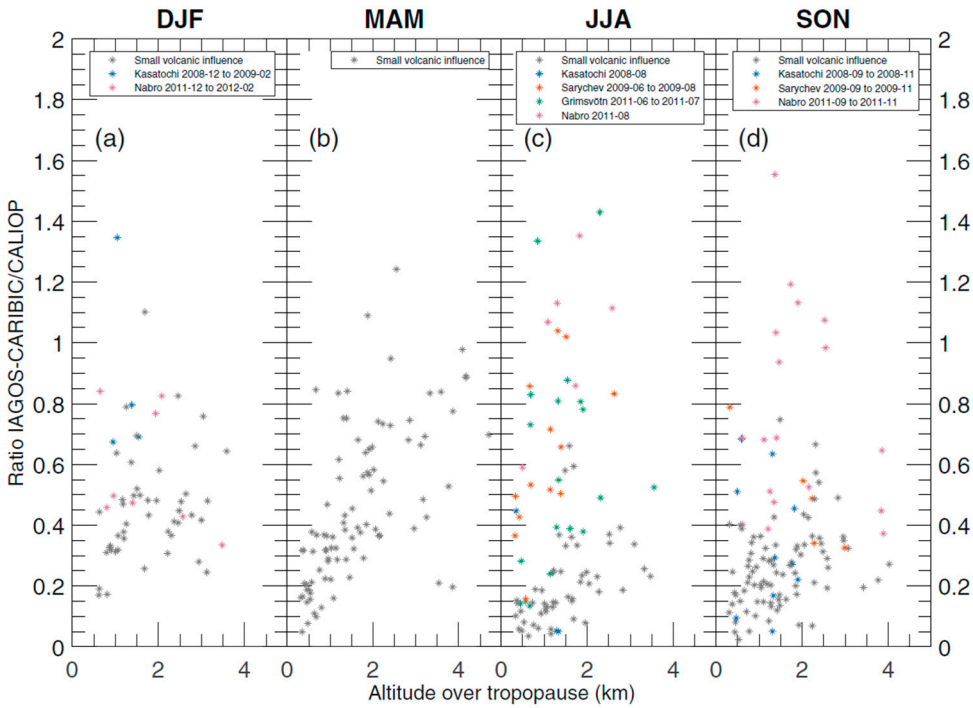

Figure 10
Ratios of the aerosol scattering measured by CALIOP and the calculated aerosol scattering based on sulphur concentrations measured by IAGOS-CARIBIC. To calculate aerosol scattering from IAGOS-CARIBIC samples, both elemental concentrations measurements as well as particle size and humidity measurements were used in the Mie scattering calculations. This is Fig. 2 in paper III.

Forest fire aerosol

The forest fires known as Great Divides fire (December, 2006) and Fire in Victoria, Australia (February, 2009) are visible in Fig. 9 in January 2007 and April 2009 in the southern hemisphere of the respective subfigures. The Great Divides fire is hard to see in the figure as the tropical volcano Rabaul erupts before the fire. The Victoria fire on the other hand is clearly visible as a red mark as it is sufficiently later after the 2008 Kasatochi eruption in order to avoid confusion. These forest fires have a minor effect on the scattering properties of the stratospheric aerosol compared to the volcanic eruptions.

No major fire events were seen in the CALIOP data until the August 2017 North American wildfires, which were studied in detail as part of this thesis. The fires produced the largest scattering and aerosol mass injected into the stratosphere ever measured by satellites (Khaykin et al., 2018;Peterson et al., 2018). The effect of these fires on the AOD is shown in Fig. 11. In Fig. 11a, the increase of AOD from background levels clearly follows after the fires. To get a comparative grasp of the size of this effect, it was compared to moderate volcanic eruptions, see Fig. 11b. In this comparison, the forest fire in North America in the year 2017 was found to increase stratospheric AOD to levels similar to volcanic eruptions. As the fire particles are already formed before the injection into the stratosphere, the AOD rises much quicker than after an eruption as the volcanic sulphate particles take time to form. However, the elevated AOD from the forest fire decreased towards background conditions faster than elevated AOD from volcanic eruptions. This could be interpreted as oxidation and evaporation of the organic particles. An even larger fire event took place around new Year 2019/2020.

The massive forest fires in recent years have both increased air pollution levels close to the surface but also released soot and organic particles into the stratosphere. Therefore, forest fires can be a source for carbon in the stratosphere and perhaps an increasingly important source for the stratospheric aerosol particles. Since the soot particles are different than both the background and volcanic particles, one would expect them to evolve differently. Organic particles are also present in the background stratospheric aerosol (Murphy et al., 2014;Martinsson et al., 2019).

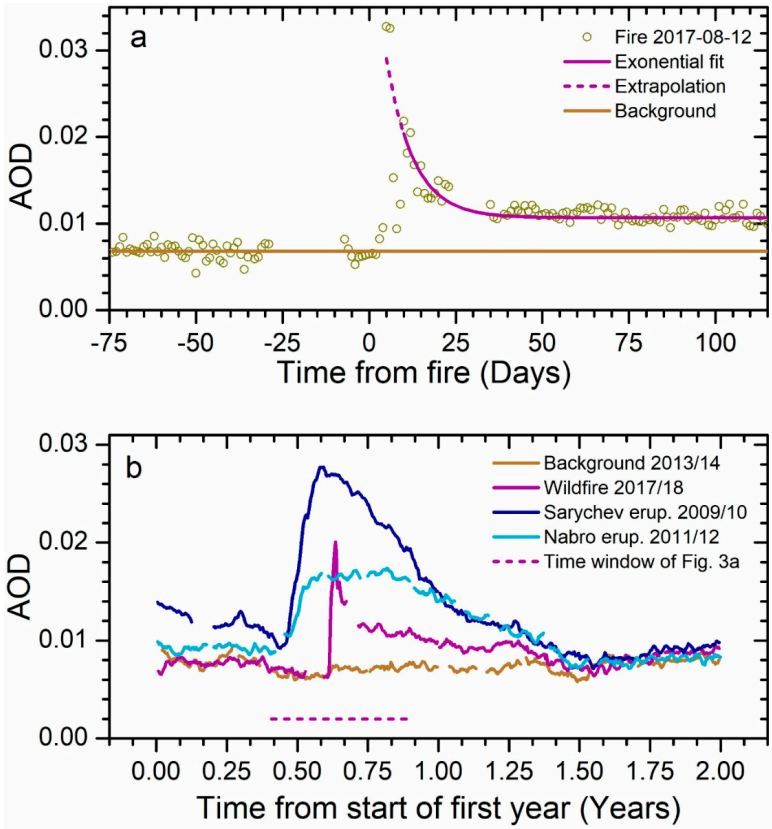

Figure 11
The evolution of AOD following the forest fires in North America in year 2017, and volcanic eruptions of Sarychev and Nabro. This figure contains results from Paper IV.

Vertical structure

In many cases, the altitude reached by a volcanic plume is reported as a single height. However, the gases are vertically distributed. By taking this into account a more detailed description of the emitted gases could be provided. Unfortunately, satellite instruments capable of observing the volcanic gases have poor vertical resolution and the instruments with high vertical resolution have not been able to observe volcanic gases directly. As the volcanic sulphate aerosol is formed out of the released volcanic gases, the aerosol can be assumed to be co-located with the released SO_2 gas. As different satellites instruments are aboard different satellites, the same air mass is measured at different areas by the satellite instruments over time. Therefore, the measurements would need to be combined.

A new method for determining the heights of volcanic SO_2 clouds has been developed for paper V. The process uses a large set of CALIOP observations of fresh aerosol from a volcanic eruption. These observations are taken over the course of several days when the aerosol is clear in individual satellite swaths. These observations of the aerosol scattering are then released into FLEXPART simulations. With the FLEXPART simulations, the air mass containing the aerosol scattering are transported to the time and locations of when the air mass has been observed by a passive satellite that lack vertical resolution but which measures SO_2 column densities. The transported aerosol scattering together with the SO_2 observations are then used to create vertical profiles of SO_2 under the assumption that the SO_2 is located at the same height as the aerosol scattering. As AIRS measurements of SO_2 are mainly sensitive to SO_2 in the upper troposphere and the stratosphere, the risk of unintentionally reporting low altitude SO_2 as stratospheric SO_2 is small.

The results from using this method are shown in Fig. 12. The figure shows the location of the volcanic SO_2 from the 2009 Sarychev eruption during one night several days after the eruption. The vertical profiles of the SO_2 are shown in Figs. 12b-d (using different height coordinates) for the AIRS swaths that contains the most SO_2 mass. It is noteworthy that the AIRS swaths closer to North America are located at higher altitudes than the AIRS swaths over northeast Asia. To compare the vertical profiles with those from other studies, the profiles were further combined into a single profile in order to aid the comparison. An early comparison shows that our method places the SO_2 at slightly higher altitudes than what the other studies have reported.

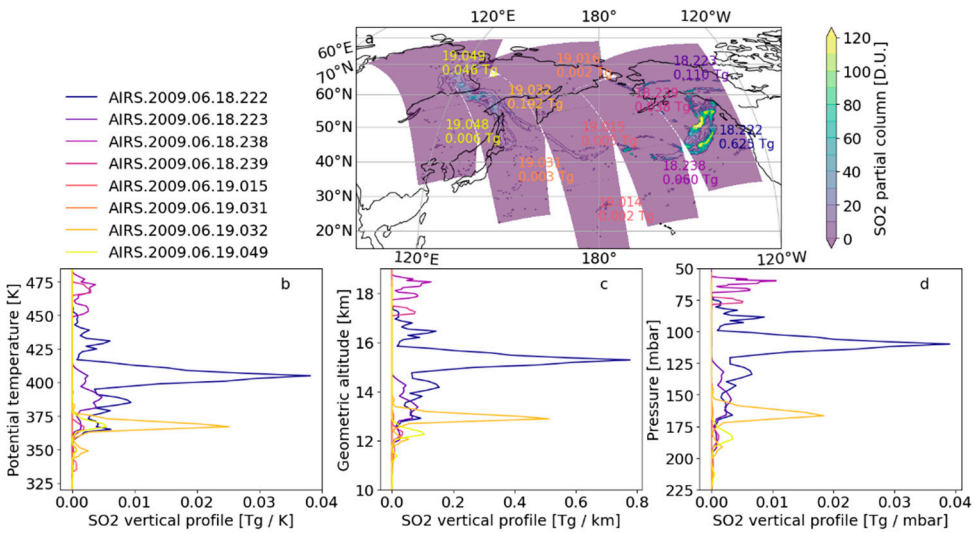

Figure 12
(a) The partial SO_2 column densities observed with the AIRS instrument. (b-d) The produced vertical profiles for the swaths with the most SO_2 mass. This is Fig. 6 in paper V.

Conclusion

The formation of the background aerosol was studied using almost a decade of elemental concentration measurements from IAGOS-CARIBIC. Additionally, comparisons between the IAGOS-CARIBIC measurements and the aerosol scattering measurements by the CALIOP lidar showed that additional components than sulphuric acid, water and organic carbon are needed to explain the observed scattering.

The long-term effects of volcanism on the stratospheric aerosol was studied by using CALIOP measurements up to the year 2015 in one of the papers in this thesis. It was found that volcanic eruptions were responsible for increasing the stratospheric aerosol optical depth by 40 % in the studied period.

Two different satellite datasets were combined through trajectory modelling to produce a SO_2 dataset with a high resolution, both in the horizontal but also the vertical dimension. The method for doing this was developed in the final paper of this thesis. The 2009 Sarychev eruption was used in this study. This eruption was composed of several smaller eruptions with different injection altitude. With the new method, the altitudes of the volcanic SO_2 were determined and compared to previously reported results.

The stratospheric smoke aerosol particles can reflect sunlight but are removed fairly quickly as they are more affected by chemistry and evaporation. The stratospheric forest fire aerosol is also rarer than stratospheric volcanic aerosol. The stratospheric aerosol was studied during short events, such as the forest fires in North America in 2017. It was found that the smoke rose into the stratosphere and blocked sunlight to the same degree as a moderate and high altitude volcanic emission would. However, the smoke's residence time in the stratosphere proved to be shorter lived than the aerosol particles from volcanic eruptions even though the smoke had optical depth of the same magnitude as the volcanic aerosol.

In conclusion, the stratospheric aerosol particles were investigated both through in-situ sampling and by remote sensing. This have resulted in a clearer picture of the stratospheric aerosol where the composition and injection height of new injections have been probed with high resolution. As a result of this work, unique datasets of the stratospheric aerosol has been created. By continuing the work presented in this thesis

it should be possible to better constrain the vertical distributions of SO_2 from volcanic eruption since this thesis have provided new tools for combining data from different satellites. The method created in paper V should also be applicable to new SO_2 observing satellites. This thesis has provided detailed measurements of what the stratospheric aerosol is made up of and what their sources are.

Outlook

The IAGOS-CARIBIC project is in the process of being moved to a new different aircraft. This next phase will continue the long successful run of the project.

As massive forest fires have become more common in recent years, their impact on the stratospheric aerosol will become more important. The work in paper IV has increased the understanding of smoke properties. It also presents a measure of AOD tied to forest fires which enables a better understanding of their radiative forcing and thus their impact on the global climate.

New satellite instruments have since the start of this work been launched and some will be launched in the future. Some of these are worthy of mention since they are similar to the instruments used in this thesis and are of interest when future studies are to be considered. The new instruments will make it possible to reproduce some of the studies in this thesis but with higher resolutions and new future volcanic eruptions.

TROPOMI, already launched on Sentinel-5P and started producing preliminary data (Theys et al., 2017;Theys et al., 2019). The TROPOMI instrument is the successor to OMI. The horizontal resolution is improved so that its nadir pixels are as small as 7×3.5 km^2. This allows the instrument to study volcanic emissions in high resolution. Also the minimum detection limit for SO_2 is lower with TROPOMI. The lowest levels of SO_2 that it can measure are 100 kg km^{-2}. This means that TROPOMI will be able to better observe small volcanic eruptions that might be missed by other instruments due to the dilution of their observations.

A more advanced lidar platform than CALIPSO is expected to be launched in 2021. It is called EarthCARE and it will carry a lidar with 355 nm wavelength (shorter than CALIOP). The short wavelength together with a high spectral resolution sensor will make it possible to calculate the lidar ratio. Thus, the satellite will be able to individually measure AOD and profiles of extinction coefficients. Apart from a very interesting lidar, the satellite will also carry a cloud profiling radar and a multi-spectral imager. The radar will use Doppler measurements to observe cloud velocities and the imager will have channels in the visible to the thermal infrared. See: https://earth.esa.int/web/guest/missions/esa-future-missions/earthcare

MAIA, is an instrument to be launched in 2021. The instrument and other instruments on the satellite are placed on a gimbal. The gimbal makes it possible to measure vertical profiles of atmospheric aerosol since the air masses can be scanned from several angles. This satellite aims to increase the understanding of the link between air pollution and health effects by having target areas where MAIA will make detailed observations and where epidemiological studies will be made on the ground. See: https://www.jpl.nasa.gov/missions/multi-angle-imager-for-aerosols-maia/

There have been suggestions to put small instruments for SO_2 detection on tiny satellites called CubeSats. This could solve the problem of long times between measurements and would allow for synchronized worldwide measurements if many instruments were put in orbit. See: https://www.aires.space/space-applications/

With all of these new developments, the stratosphere will have a host of new highly detailed datasets of the aerosol. Future research need to combine these measurements in novel ways. This will enable the stratospheric aerosol to be better characterized and the causal relationship between forest fires, volcanic eruptions and the global climate to be better understood. This increased understanding will enable climate models to become more accurate and to better incorporate effects from volcanic eruptions and fire events.

References

Andersson, S. M., Martinsson, B. G., Vernier, J. P., Friberg, J., Brenninkmeijer, C. A. M., Hermann, M., van Velthoven, P. F. J., and Zahn, A.: Significant radiative impact of volcanic aerosol in the lowermost stratosphere, Nat. Commun., 10.1038/ncomms8692, 2015.

Appenzeller, C., Holton, J. R., and Rosenlof, K. H.: Seasonal variation of mass transport across the tropopause, J. Geophys. Res., 101, 15071-15078, 1996.

Bourassa, A. E., Rieger, L. A., Zawada, D. J., Khaykin, S., Thomason, L. W., and Degenstein, D. A.: Satellite Limb Observations of Unprecedented Forest Fire Aerosol in the Stratosphere, J. Geophys. Res. Atmos., 124, 9510-9519, 10.1029/2019jd030607, 2019.

Brenninkmeijer, C. A. M., Crutzen, P., Boumard, F., Dauer, T., Dix, B., Ebinghaus, R., Filippi, D., Fischer, H., Franke, H., Frieß, U., and Heintzenberg, J.: Civil Aircraft for the regular investigation of the atmosphere based on an instrumented container: The new CARIBIC system, Atmos. Chem. Phys., 7, 4953-4976, 2007.

Butchart, N.: The Brewer-Dobson circulation, Rev. Geophys., 52, 157-184, 10.1002/2013rg000448, 2014.

Carn, S. A., Pallister, J. S., Lara, L., Ewert, J. W., Watt, S., Prata, A. J., Thomas, R. J., and Villarosa, G.: The Unexpected Awakening of Chaitén Volcano, Chile, Eos, Transactions American Geophysical Union, 90, 205-206, https://doi.org/10.1029/2009EO240001, 2009.

Carn, S. A., and Prata, F. J.: Satellite-based constraints on explosive SO2 release from Soufrière Hills Volcano, Montserrat, Geophys. Res. Lett., 37, L00E22, 10.1029/2010GL044971, 2010.

Carn, S. A.: On the detection and monitoring of effusive eruptions using satellite SO2 measurements, Geological Society, London, Special Publications, 426, 277-292, 10.1144/sp426.28, 2016.

Clarisse, L., Hurtmans, D., Clerbaux, C., Hadji-Lazaro, J., Ngadi, Y., and Coheur, P.-F.: Retrieval of sulphur dioxide from the infrared atmospheric sounding interferometer (IASI), Atmos. Meas. Tech., 5, 581-594, 10.5194/amt-5-581-2012, 2012.

de Laat, A. T. J., Stein Zweers, D. C., Boers, R., and Tuinder, O. N. E.: A solar escalator: Observational evidence of the self-lifting of smoke and aerosols by absorption of solar radiation in the February 2009 Australian Black Saturday plume, J. Geophys. Res. Atmos., 117, 10.1029/2011jd017016, 2012.

Deshler, T.: A review of global stratospheric aerosol: Measurements, importance, life cycle, and local stratospheric aerosol, Atmos. Res., 90, 223-232, 2008.

Diallo, M., Ploeger, F., Konopka, P., Birner, T., Müller, R., Riese, M., Garny, H., Legras, B., Ray, E., Berthet, G., and Jegou, F.: Significant Contributions of Volcanic Aerosols to Decadal Changes in the Stratospheric Circulation, Geophys. Res. Lett., 44, 10,780-710,791, 10.1002/2017gl074662, 2017.

Fioletov, V., McLinden, C. A., Kharol, S. K., Krotkov, N. A., Li, C., Joiner, J., Moran, M. D., Vet, R., Visschedijk, A. J. H., and Denier van der Gon, H. A. C.: Multi-source SO2 emission retrievals and consistency of satellite and surface measurements with reported emissions, Atmos. Chem. Phys, 17, 12597-12616, 10.5194/acp-17-12597-2017, 2017.

Flemming, J., and Inness, A.: Volcanic sulfur dioxide plume forecasts based on UV satellite retrievals for the 2011 Grímsvötn and the 2010 Eyjafjallajökull eruption, J. Geophys. Res. Atmos., 118, 10,172-110,189, 10.1002/jgrd.50753, 2013.

Friberg, J., Martinsson, B. G., Andersson, S. M., and Sandvik, O. S.: Volcanic impact on the climate – the stratospheric aerosol load in the period 2006–2015, Atmos. Chem. Phys, 18, 11149-11169, 10.5194/acp-18-11149-2018, 2018.

Ge, C., Wang, J., Carn, S., Yang, K., Ginoux, P., and Krotkov, N.: Satellite-based global volcanic SO2 emissions and sulfate direct radiative forcing during 2005-2012, J. Geophys. Res. Atmos., 121, 3446-3464, 10.1002/2015jd023134, 2016.

Gettelman, A., Hoor, P., Pan, L. L., Randel, W. J., Hegglin, M. I., and Birner, T.: The Extratropical Upper Troposphere and Lower Stratosphere, Rev. Geophys., 49, RG3003, 10.1029/2011rg000355, 2011.

Gordon, I. E., Rothman, L. S., Hill, C., Kochanov, R. V., Tan, Y., Bernath, P. F., Birk, M., Boudon, V., Campargue, A., Chance, K. V., Drouin, B. J., Flaud, J. M., Gamache, R. R., Hodges, J. T., Jacquemart, D., Perevalov, V. I., Perrin, A., Shine, K. P., Smith, M. A. H., Tennyson, J., Toon, G. C., Tran, H., Tyuterev, V. G., Barbe, A., Császár, A. G., Devi, V. M., Furtenbacher, T., Harrison, J. J., Hartmann, J. M., Jolly, A., Johnson, T. J., Karman, T., Kleiner, I., Kyuberis, A. A., Loos, J., Lyulin, O. M., Massie, S. T., Mikhailenko, S. N., Moazzen-Ahmadi, N., Müller, H. S. P., Naumenko, O. V., Nikitin, A. V., Polyansky, O. L., Rey, M., Rotger, M., Sharpe, S. W., Sung, K., Starikova, E., Tashkun, S. A., Auwera, J. V., Wagner, G., Wilzewski, J., Wcisło, P., Yu, S., and Zak, E. J.: The HITRAN2016 molecular spectroscopic database, Journal of Quantitative Spectroscopy and Radiative Transfer, 203, 3-69, 10.1016/j.jqsrt.2017.06.038, 2017.

Haynes, P., and Shuckburgh, E.: Effective diffusivity as a diagnostic of atmospheric transport 2. Troposphere and lower stratosphere, J. Geophys. Res., 105, 22795-22810, 2000.

Haywood, J. M., Clerbaux, C., Coheur, P., Degenstein, D., Braesicke, P., Jones, A., Clarisse, L., Bourassa, A., Barnes, J., Telford, P., Bellouin, N., Boucher, O., and Agnew, P.: Observations of the eruption of the Sarychev volcano and simulations using the HadGEM2 climate model, J. Geophys. Res., 115, D21212, 10.1029/2010JD014447, 2010.

Heard, I. P. C., Manning, A. J., Haywood, J. M., Witham, C., Redington, A., Jones, A., Clarisse, L., and Bourassa, A.: A comparison of atmospheric dispersion model predictions with observations of SO2

and sulphate aerosol from volcanic eruptions, J. Geophys. Res. Atmos., 117, 10.1029/2011jd016791, 2012.

Hermann, M., Weigelt, A., Assmann, D., Pfeifer, S., Müller, T., Conrath, T., Voigtländer, J., Heintzenberg, J., Wiedensohler, A., Martinsson, B. G., Deshler, T., Brenninkmeijer, C. A. M., and Zahn, A.: An optical particle size spectrometer for aircraft-borne measurements in IAGOS-CARIBIC, Atmos. Meas. Tech., 9, 2179-2194, 10.5194/amt-9-2179-2016, 2016.

Hersbach, H., Bell, B., Berrisford, P., Hirahara, S., Horányi, A., Muñoz-Sabater, J., Nicolas, J., Peubey, C., Radu, R., Schepers, D., Simmons, A., Soci, C., Abdalla, S., Abellan, X., Balsamo, G., Bechtold, P., Biavati, G., Bidlot, J., Bonavita, M., Chiara, G., Dahlgren, P., Dee, D., Diamantakis, M., Dragani, R., Flemming, J., Forbes, R., Fuentes, M., Geer, A., Haimberger, L., Healy, S., Hogan, R. J., Hólm, E., Janisková, M., Keeley, S., Laloyaux, P., Lopez, P., Lupu, C., Radnoti, G., Rosnay, P., Rozum, I., Vamborg, F., Villaume, S., and Thépaut, J. N.: The ERA5 global reanalysis, Q. J. Roy. Meteor. Soc., 146, 1999-2049, 10.1002/qj.3803, 2020.

Hofmann, D. J., and Solomon, S.: Ozone destruction through heterogeneous chemistry following the eruption of El Chichón, J. Geophys. Res., 94, 5029-5041, 1989.

Hoor, P., Fischer, H., and Lelieveld, J.: Tropical and extratropical tropospheric air in the lowermost stratosphere over Europe: A CO-based budget, Geophys. Res. Lett., 32, 10.1029/2004GL022018, 2005.

Hoskins, B. J.: Towards a PV-θ view of the general circulation, Tellus, Ser AB, 43, 27-35, 1991.

Hou, P., and Wu, S.: Long-term Changes in Extreme Air Pollution Meteorology and the Implications for Air Quality, Sci Rep, 6, 23792, 10.1038/srep23792, 2016.

IPCC: Anthropogenic and Natural Radiative Forcing. In: Climate Change 2013: The Physical Science Basis. Contribution of Working Group I to the Fifth Assessment Report of the Intergovernmental Panel on Climate Change, Cambridge University Press, Cambridge, United Kingdom and New York, NY, USA, 1535, 2013.

Jacob, D. J.: Introduction to atmospheric chemistry, Princeton University Press, New Jersey, 1999.

Kar, J., Vaughan, M. A., Lee, K.-P., Tackett, J. L., Avery, M. A., Garnier, A., Getzewich, B. J., Hunt, W. H., Josset, D., Liu, Z., Lucker, P. L., Magill, B., Omar, A. H., Pelon, J., Rogers, R. R., Toth, T. D., Trepte, C. R., Vernier, J.-P., Winker, D. M., and Young, S. A.: CALIPSO lidar calibration at 532 nm: version 4 nighttime algorithm, Atmos. Meas. Tech., 11, 1459-1479, 10.5194/amt-11-1459-2018, 2018.

Khaykin, S. M., Godin-Beekmann, S., Hauchecorne, A., Pelon, J., Ravetta, F., and Keckhut, P.: Stratospheric Smoke With Unprecedentedly High Backscatter Observed by Lidars Above Southern France, Geophys. Res. Lett., 45, 1639-1646, 10.1002/2017gl076763, 2018.

Kremser, S., Thomason, L. W., von Hobe, M., Hermann, M., Deshler, T., Timmreck, C., Toohey, M., Stenke, A., Schwarz, J. P., Weigel, R., Fueglistaler, S., Prata, F. J., Vernier, J.-P., Schlager, H., Barnes, J. E., Antuña-Marrero, J.-C., Fairlie, D., Palm, M., Mahieu, E., Notholt, J., Rex, M., Bingen, C., Vanhellemont, F., Bourassa, A., Plane, J. M. C., Klocke, D., Carn, S. A., Clarisse, L., Trickl, T., Neely, R., James, A. D., Rieger, L., Wilson, J. C., and Meland, B.: Stratospheric aerosol-Observations, processes, and impact on climate, Rev. Geophys., 54, 278-335, 10.1002/2015rg000511, 2016.

Kristiansen, N. I., Stohl, A., Prata, A. J., Richter, A., Eckhardt, S., Seibert, P., Hoffmann, A., Ritter, C., Bitar, L., Duck, T. J., and Stebel, K.: Remote sensing and inverse transport modeling of the Kasatochi eruption sulfur dioxide cloud, J. Geophys. Res., 115, 10.1029/2009jd013286, 2010.

Kristiansen, N. I., Prata, A. J., Stohl, A., and Carn, S. A.: Stratospheric volcanic ash emissions from the 13 February 2014 Kelut eruption, Geophys. Res. Lett., 42, 588-596, 10.1002/2014gl062307, 2015.

Lee, C., Martin, R. V., van Donkelaar, A., O'Byrne, G., Krotkov, N., Richter, A., Huey, L. G., and Holloway, J. S.: Retrieval of vertical columns of sulfur dioxide from SCIAMACHY and OMI: Air mass factor algorithm development, validation, and error analysis, J. Geophys. Res., 114, 10.1029/2009jd012123, 2009.

LeGrande, A. N., Tsigaridis, K., and Bauer, S. E.: Role of atmospheric chemistry in the climate impacts of stratospheric volcanic injections, Nat. Geosci., 9, 652-655, 10.1038/ngeo2771, 2016.

Lelieveld, J., Bregman, B., Arnold, F., Bürger, V., Crutzen, P. J., Fischer, H., Waibel, A., Siegmund, P., and Van Velthoven, P. F. J.: Chemical perturbation of the lowermost stratosphere through exchange with the troposphere, Geophys. Res. Lett., 24, 603-606, 1997.

Lelieveld, J., Evans, J. S., Fnais, M., Giannadaki, D., and Pozzer, A.: The contribution of outdoor air pollution sources to premature mortality on a global scale, Nature, 525, 367-371, 10.1038/nature15371, 2015.

Lelieveld, J., Klingmuller, K., Pozzer, A., Burnett, R. T., Haines, A., and Ramanathan, V.: Effects of fossil fuel and total anthropogenic emission removal on public health and climate, Proc Natl Acad Sci U S A, 116, 7192-7197, 10.1073/pnas.1819989116, 2019.

Li, C., Krotkov, N. A., Carn, S., Zhang, Y., Spurr, R. J. D., and Joiner, J.: New-generation NASA Aura Ozone Monitoring Instrument (OMI) volcanic SO2 dataset: algorithm description, initial results, and continuation with the Suomi-NPP Ozone Mapping and Profiler Suite (OMPS), Atmos. Meas. Tech., 10, 445-458, 10.5194/amt-10-445-2017, 2017.

Lopez, T., Carn, S. A., Werner, C. A., Fee, D., Kelly, P., Doukas, M., Pfeffer, M., Webley, P., Cahill, C., and Schneider, D.: Evaluation of Redoubt Volcano's sulfur dioxide emissions by the Ozone Monitoring Instrument, J. Volcanol. and Geoth. Res., 259, 290-307, 10.1016/j.jvolgeores.2012.03.002, 2013.

Martinsson, B. G., Nguyen, H. N., Brenninkmeijer, C. A., Zahn, A., Heintzenberg, J., Hermann, M., and Van Velthoven, P. F.: Characteristics and origin of lowermost stratospheric aerosol at northern midlatitudes under volcanically quiescent conditions based on CARIBIC observations, J. Geophys Res., 110, D12201, 10.1029/2004jd005644, 2005.

Martinsson, B. G., Friberg, J., Andersson, S. M., Weigelt, A., Hermann, M., Assmann, D., Voigtländer, J., Brenninkmeijer, C. A. M., Velthoven, P. J. F. v., and Zahn, A.: Comparison between CARIBIC aerosol samples analysed by accelerator-based methods and optical particle counter measurements, Atmos. Meas. Tech., 7, 2581-2596, 10.5194/amt-7-2581-2014, 2014.

Martinsson, B. G., Friberg, J., Sandvik, O. S., Hermann, M., van Velthoven, P. F. J., and Zahn, A.: Formation and composition of the UTLS aerosol, npj Climate and Atmospheric Science, 2, 10.1038/s41612-019-0097-1, 2019.

Mattis, I., Siefert, P., Müller, D., Tesche, M., Hiebsch, A., Kanitz, T., Schmidt, J., Finger, F., Wandinger, U., and Ansmann, A.: Volcanic aerosol layers observed with multiwavelength Raman lidar over central Europe in 2008–2009, J. Geophys. Res., 115, 10.1029/2009jd013472, 2010.

McCormick, M. P., Thomason, L. W., and Trepte, C. R.: Atmospheric effects of the Mt Pinatubo eruption, Nature, 373, 399-404, 1995.

Murphy, D. M., Thomson, D. S., and Mahoney, M. J.: In situ measurements of organics, meteoritic material, mercury, and other elements in aerosols at 5 to 19 kilometers, Science, 282, 1664-1669, 10.1126/science.282.5394.1664, 1998.

Murphy, D. M., Froyd, K. D., Schwarz, J. P., and Wilson, J. C.: Observations of the chemical composition of stratospheric aerosol particles, Q. J. R. Meteorol. Soc., 140, 1269–1278, 2014.

Nguyen, N. H., Gudmundsson, A., and Martinsson, B.: Design and calibration of a multi-channel aerosol sampler for tropopause region studies from the CARIBIC platform, Aerosol Sci. Tech., 40, 649-655, 10.1080/02786820600767807, 2006.

Olson, D. W., Doescher, R. L., and Olson, M. S.: When the Sky Ran Red The Story Behind the Scream, Sky & Telescope, 2004.

Papaspiropoulos, G., Mentes, B., Kristiansson, P., and Martinsson, B. G.: A high sensitivity elemental analysis methodology for upper tropospheric aerosol, Nucl. Instrum. Methods Phys. Res., Sect. B, 150, 356-362, 1999.

Pardini, F., Burton, M., Arzilli, F., La Spina, G., and Polacci, M.: Satellite-derived SO2 flux time-series and magmatic processes during the 2015 Calbuco eruptions, Solid Earth Discuss., 2017, 1-25, 10.5194/se-2017-64, 2017.

Peterson, D. A., Campbell, J. R., Hyer, E. J., Fromm, M. D., Kablick, G. P., 3rd, Cossuth, J. H., and DeLand, M. T.: Wildfire-driven thunderstorms cause a volcano-like stratospheric injection of smoke, NPJ Clim Atmos Sci, 1, 10.1038/s41612-018-0039-3, 2018.

Pisso, I., Sollum, E., Grythe, H., Kristiansen, N. I., Cassiani, M., Eckhardt, S., Arnold, D., Morton, D., Thompson, R. L., Groot Zwaaftink, C. D., Evangeliou, N., Sodemann, H., Haimberger, L., Henne, S., Brunner, D., Burkhart, J. F., Fouilloux, A., Brioude, J., Philipp, A., Seibert, P., and Stohl, A.: The Lagrangian particle dispersion model FLEXPART version 10.4, Geoscientific Model Development, 12, 4955-4997, 10.5194/gmd-12-4955-2019, 2019.

Prata, A. J., and Bernardo, C.: Retrieval of volcanic SO_2 column abundance from atmospheric infrared sounder data, J. Geophys. Res., 112, D20204, 10.1029/2006JD007955, 2007.

Prata, A. J., Gangale, G., Clarisse, L., and Karagulian, F.: Ash and sulfur dioxide in the 2008 eruptions of Okmok and Kasatochi: Insights from high spectral resolution satellite measurements, J. Geophys. Res., 115, 10.1029/2009jd013556, 2010.

Prata, A. T., Young, S. A., Siems, S. T., and Manton, M. J.: Lidar ratios of stratospheric volcanic ash and sulfate aerosols retrieved from CALIOP measurements, Atmos. Chem. Phys, 17, 8599-8618, 10.5194/acp-17-8599-2017, 2017.

Ramanathan, V., and Carmichael, G.: Global and regional climate changes due to black carbon, Nat. Geosci., 1, 221-227, 10.1038/ngeo156, 2008.

Robock, A.: Volcanic eruptions and climate, Rev. Geophys., 38, 191-219, 2000.

Sandvik, O. S., Friberg, J., Martinsson, B. G., van Velthoven, P. F. J., Hermann, M., and Zahn, A.: Intercomparison of in-situ aircraft and satellite aerosol measurements in the stratosphere, Sci. Rep., 9, 15576, 10.1038/s41598-019-52089-6, 2019.

Santer, B. D., Bonfils, C., Painter, J. F., Zelinka, M. D., Mears, C., Solomon, S., Schmidt, G. A., Fyfe, J. C., Cole, J. N. S., and Nazarenko, L.: Volcanic contribution to decadal changes in tropospheric temperature, Nat. Geosci., 7, 185-189, 2014.

Sheng, J.-X., Weisenstein, D. K., Luo, B.-P., Rozanov, E., Stenke, A., Anet, J., Bingemer, H., and Peter, T.: Global atmospheric sulfur budget under volcanically quiescent conditions: Aerosol-chemistry-climate model predictions and validation, J. Geophys. Res. Atmos., 120, 256-276, 10.1002/2014jd021985, 2015.

Stohl, A., Forster, C., Frank, A., Seibert, P., and Wotawa, G.: Technical note The Lagrangian particle dispersion model FLEXPART version 6.2, Atmos. Chem. Phys., 5, 2461-2474, 2005.

Stratosphere-troposphere Processes and their Role in Climate (SPARC): SPARC Assessment of Stratospheric Aerosol Properties (ASAP), SPARC Report, 2006, 322 pp.,

Sumpf, B.: Line intensity and self-broadening investigations in the ν1 and ν3 bands of SO2, Journal of Molecular Structure, 599, 39-49, 2001.

Surono, Jousset, P., Pallister, J., Boichu, M., Buongiorno, M. F., Budisantoso, A., Costa, F., Andreastuti, S., Prata, F., Schneider, D., and Clarisse, L.: The 2010 explosive eruption of Java's Merapi volcano—a '100-year'event, J. Volcanol. and Geoth. Res., 121-135, 10.1016/j.jvolgeores.2012.06.018, 2012.

Theys, N., Campion, R., Clarisse, L., Brenot, H., van Gent, J., Dils, B., Corradini, S., Merucci, L., Coheur, P. F., Van Roozendael, M., Hurtmans, D., Clerbaux, C., Tait, S., and Ferrucci, F.: Volcanic SO2 fluxes derived from satellite data: a survey using OMI, GOME-2, IASI and MODIS, Atmos. Chem. Phys, 13, 5945-5968, 10.5194/acp-13-5945-2013, 2013.

Theys, N., De Smedt, I., Yu, H., Danckaert, T., van Gent, J., Hörmann, C., Wagner, T., Hedelt, P., Bauer, H., Romahn, F., Pedergnana, M., Loyola, D., and Van Roozendael, M.: Sulfur dioxide retrievals from TROPOMI onboard Sentinel-5 Precursor: algorithm theoretical basis, Atmos. Meas. Tech., 10, 119-153, 10.5194/amt-10-119-2017, 2017.

Theys, N., Hedelt, P., De Smedt, I., Lerot, C., Yu, H., Vlietinck, J., Pedergnana, M., Arellano, S., Galle, B., Fernandez, D., Carlito, C. J. M., Barrington, C., Taisne, B., Delgado-Granados, H., Loyola, D., and Van Roozendael, M.: Global monitoring of volcanic SO2 degassing with unprecedented resolution from TROPOMI onboard Sentinel-5 Precursor, Sci Rep, 9, 2643, 10.1038/s41598-019-39279-y, 2019.

Thomas, H. E., Watson, I. M., Carn, S. A., Prata, A. J., and Realmuto, V. J.: A comparison of AIRS, MODIS and OMI sulphur dioxide retrievals in volcanic clouds, Geomat. Nat. Haz. Risk, 2, 217-232, 10.1080/19475705.2011.564212, 2011.

Thomason, L., and Vernier, J.-P.: Improved SAGE II cloud/aerosol categorization and observations of the Asian tropopause aerosol layer: 1989–2005, Atm. Chem. Phys., 13, 4605-4616, 10.5194/acp-13-4605-2013, 2013.

Vernier, J. P., Pommereau, J. P., Garnier, A., Pelon, J., Larsen, N., Nielsen, J., Christensen, T., Cairo, F., Thomason, L. W., Leblanc, T., and McDermid, I. S.: Tropical stratospheric aerosol layer from CALIPSO lidar observations, J. Geophys Res., 114, D00H10, 10.1029/2009jd011946, 2009.

Vernier, J. P., Thomason, L. W., and Kar, J.: CALIPSO detection of an Asian tropopause aerosol layer, Geophys. Res. Lett., 38, L07804, 10.1029/2010GL046614, 2011.

Vernier, J. P., Fairlie, T. D., Natarajan, M., Wienhold, F. G., Bian, J., Martinsson, B. G., Crumeyrolle, S., Thomason, L. W., and Bedka, K. M.: Increase in upper tropospheric and lower stratospheric aerosol levels and its potential connection with Asian pollution, J. Geophys. Res. Atmos., 120, 1608-1619, 10.1002/2014JD022372, 2015.

Vernier, J. P., Fairlie, T. D., Deshler, T., Venkat Ratnam, M., Gadhavi, H., Kumar, B. S., Natarajan, M., Pandit, A. K., Akhil Raj, S. T., Hemanth Kumar, A., Jayaraman, A., Singh, A. K., Rastogi, N., Sinha, P. R., Kumar, S., Tiwari, S., Wegner, T., Baker, N., Vignelles, D., Stenchikov, G., Shevchenko, I., Smith, J., Bedka, K., Kesarkar, A., Singh, V., Bhate, J., Ravikiran, V., Durga Rao, M., Ravindrababu, S., Patel, A., Vernier, H., Wienhold, F. G., Liu, H., Knepp, T. N., Thomason, L., Crawford, J., Ziemba, L., Moore, J., Crumeyrolle, S., Williamson, M., Berthet, G., Jégou, F., and Renard, J. B.:

BATAL: The Balloon Measurement Campaigns of the Asian Tropopause Aerosol Layer, B. Am. Meteorol. Soc., 99, 955-973, 10.1175/bams-d-17-0014.1, 2018.

Watts, N., Amann, M., Arnell, N., Ayeb-Karlsson, S., Beagley, J., Belesova, K., Boykoff, M., Byass, P., Cai, W., Campbell-Lendrum, D., Capstick, S., Chambers, J., Coleman, S., Dalin, C., Daly, M., Dasandi, N., Dasgupta, S., Davies, M., Di Napoli, C., Dominguez-Salas, P., Drummond, P., Dubrow, R., Ebi, K. L., Eckelman, M., Ekins, P., Escobar, L. E., Georgeson, L., Golder, S., Grace, D., Graham, H., Haggar, P., Hamilton, I., Hartinger, S., Hess, J., Hsu, S.-C., Hughes, N., Jankin Mikhaylov, S., Jimenez, M. P., Kelman, I., Kennard, H., Kiesewetter, G., Kinney, P. L., Kjellstrom, T., Kniveton, D., Lampard, P., Lemke, B., Liu, Y., Liu, Z., Lott, M., Lowe, R., Martinez-Urtaza, J., Maslin, M., McAllister, L., McGushin, A., McMichael, C., Milner, J., Moradi-Lakeh, M., Morrissey, K., Munzert, S., Murray, K. A., Neville, T., Nilsson, M., Sewe, M. O., Oreszczyn, T., Otto, M., Owfi, F., Pearman, O., Pencheon, D., Quinn, R., Rabbaniha, M., Robinson, E., Rocklöv, J., Romanello, M., Semenza, J. C., Sherman, J., Shi, L., Springmann, M., Tabatabaei, M., Taylor, J., Triñanes, J., Shumake-Guillemot, J., Vu, B., Wilkinson, P., Winning, M., Gong, P., Montgomery, H., and Costello, A.: The 2020 report of The Lancet Countdown on health and climate change: responding to converging crises, The Lancet, 10.1016/s0140-6736(20)32290-x, 2020.

Watts, S. F.: The mass budgets of carbonyl sulfide, dimethyl sulfide, carbon disulfide and hydrogen sulfide, Atmospheric Environment, 34, 761-779, 10.1016/s1352-2310(99)00342-8, 2000.

Winker, D. M., Vaughan, M. A., Omar, A., Hu, Y., Powell, K. A., Liu, Z., Hunt, W. H., and Young, S. A.: Overview of the CALIPSO Mission and CALIOP Data Processing Algorithms, J. Atmos. Ocean Tech., 26, 2310-2323, 10.1175/2009jtecha1281.1, 2009.

Yu, P., Toon, O. B., Neely, R. R., Martinsson, B. G., and Brenninkmeijer, C. A. M.: Composition and physical properties of the Asian Tropopause Aerosol Layer and the North American Tropospheric Aerosol Layer, Geophys. Res. Lett., 42, 2540-2546, 10.1002/2015gl063181, 2015.

Zhu, C., Kanaya, Y., Takigawa, M., Ikeda, K., Tanimoto, H., Taketani, F., Miyakawa, T., Kobayashi, H., and Pisso, I.: FLEXPART v10.1 simulation of source contributions to Arctic black carbon, Atmos. Chem. Phys, 20, 1641-1656, 10.5194/acp-20-1641-2020, 2020.